Early extension and associated mafic alkalic volcanism from the southern Basin and Range Province: Geology and petrology of the Rodeo and Nazas volcanic fields, Durango, México

James F. Luhr*
Department of Mineral Sciences, NHB-119, Smithsonian Institution, Washington, DC 20560, USA

Christopher D. Henry†
Nevada Bureau of Mines and Geology, University of Nevada, Reno, Nevada 89557, USA

Todd B. Housh§
Department of Geological Sciences, University of Texas, Austin, Texas 78712, USA

J. Jorge Aranda-Gómez#
Unidad de Investigación en Ciencias de la Tierra, Instituto de Geología, Universidad Nacional Autonoma de México, Campus Juriquilla, A.P. 1-742, Querétaro, QRO 76001, Mexico

William C. McIntosh**
New Mexico Bureau of Mines and Mineral Resources, New Mexico Institute of Mining and Technology, P.O. Box 3398 Campus Station, Socorro, New Mexico 87801, USA

ABSTRACT

East-northeast extension ca. 24 Ma at Rodeo and Nazas, México, was accompanied by eruption of hawaiites, marking some of the earliest intraplate-type mafic alkalic volcanism associated with development of the southern Basin and Range Province. An earlier extensional pulse, 32.3–30.6 Ma, concurrent with subduction-related rhyolitic volcanism of the Sierra Madre Occidental, is the earliest established extension in the southern Basin and Range Province. The Rodeo hawaiites are mostly along or just west of the north-northwest–striking, west-dipping Rodeo fault, a major breakaway fault that separates moderately extended terrane to the west from less extended terrane to the east. Hawaiites and interbedded conglomerates in the Rodeo half graben are flat lying to gently tilted and cut by the Rodeo fault. Underlying Eocene–Oligocene ash-flow tuffs to the west are cut by numerous west-dipping faults and tilted as much as 40°. Nazas hawaiites are also along north-northwest–striking faults but are generally unfaulted.

Like other Miocene mafic alkalic volcanic rocks from the southern Basin and Range Province, those from Rodeo and Nazas are characterized by (1) moderately evolved hawaiitic compositions, (2) abundant megacrysts, including sodic plagioclase ($An_{26–51}$), olivine ($\sim Fo_{55}$), Al-augite (7–9 wt% Al_2O_3), and a wide variety of spinels, (3) lack of granulitic or peridotitic xenoliths, (4) variable Cs enrichments, and (5) isotopic compositions that indicate interaction with crust ($^{87}Sr/^{86}Sr_i = 0.7037–0.7041$; $\epsilon_{Nd} = 4.8–2.8$; $^{206}Pb/^{204}Pb_i = 18.91–18.77$; $^{207}Pb/^{204}Pb_i = 15.57–15.60$). These observations are consistent with a model whereby Miocene intraplate-type magmas rose slowly through the lithosphere, differentiating and interacting with the crust. The megacrysts are interpreted as disrupted gabbroic bodies, formed by slow cooling of mafic alkalic magmas that stagnated in the lower crust, possibly during the earlier extensional episode. Many of the elemental and isotopic parameters used to probe mantle sources of mafic volcanic rocks have been seriously obscured by crystallization, crustal interaction, and megacryst incorporation, complicating efforts to identify temporal changes in mantle source regions during development of the southern Basin and Range Province.

Keywords: Basin and Range province, contamination (magma), Durango Mexico, extension faults, hawaiite, Miocene.

INTRODUCTION

Continental rifting is one of Earth's fundamental geological processes. Whether ultimately driven by crustal tectonics or deeper mantle-flow phenomena, current models for continental rifting invoke thinning of the lithospheric mantle and crust accompanied by ascent of convecting upper mantle beneath the rift. Geochemical studies of mafic volcanic rocks from the Rio Grande rift area (Perry et al., 1987, 1988) and from the Colorado River trough (Daley and DePaolo, 1992; Bradshaw et al., 1993) in the United States portion of the Basin and Range Province have identified temporal changes in Nd and Sr isotopic compositions and other geochemical parameters. These changes have been used to infer that mantle source regions migrated with time from the shallower lithospheric mantle (high $^{87}Sr/^{86}Sr$, low ϵ_{Nd}) to the deeper convecting as-

*E-mail: luhr@volcano.si.edu.
†E-mail: chenry@nbmg.unr.edu.
§E-mail: housh@mail.utexas.edu.
#E-mail: jjag@servidor.unam.mx.
**E-mail: mcintosh@nmt.edu.

GSA Bulletin; June 2001; v. 113; no. 6; p. 760–773; 8 figures; 4 tables; Data Repository item 2001060.

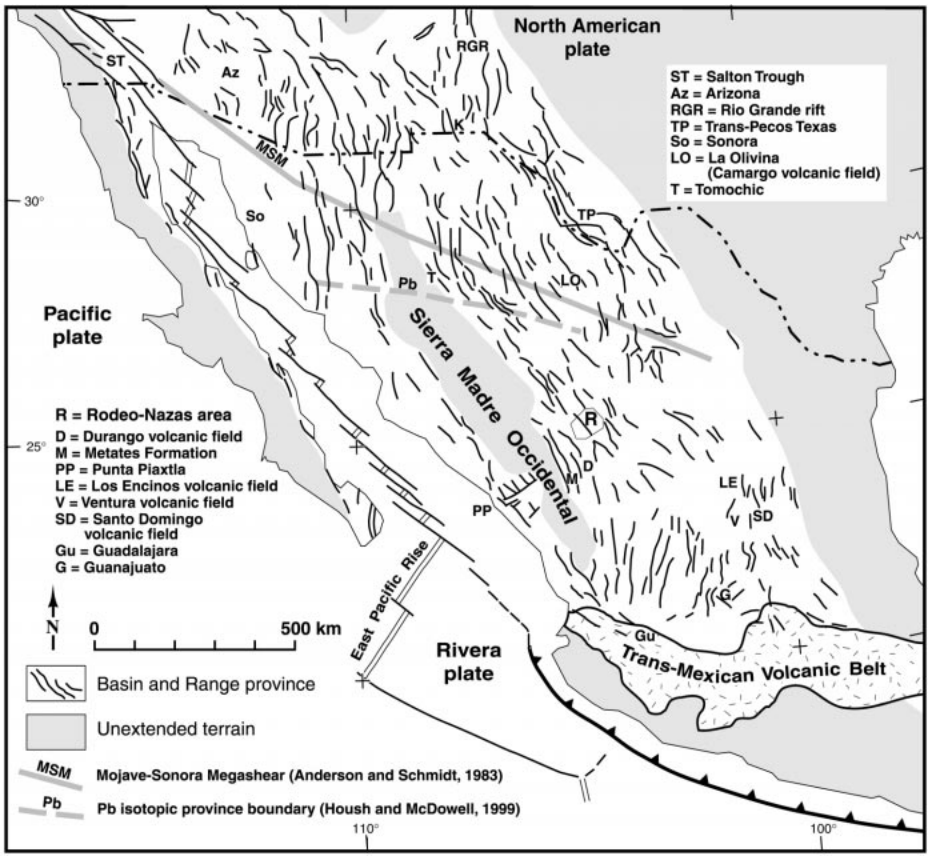

Figure 1. The southern Basin and Range Province of México, showing generalized mid-late Cenozoic fault patterns and location of the Rodeo-Nazas area (R: polygon shows the area of Fig. 2) (Henry and Aranda-Gómez, 1992, 2000; Aranda-Gómez et al., 1997; Stewart et al., 1998). The Rodeo-Nazas area is ~100 km east of the unextended structural core of the Sierra Madre Occidental but within the area of mid-Cenozoic ignimbrites of the Sierra Madre volcanic province. The boundary between basement provinces based on Pb isotopic ratios proposed by Housh and McDowell (1999) is shown as a dashed line north of Rodeo and Nazas.

thenospheric mantle (low $^{87}Sr/^{86}Sr$, high ϵ_{Nd}). Other studies, however, have emphasized the cryptic nature of crustal contamination (Doe et al., 1969; Glazner and Farmer, 1992; Baldridge et al., 1996), which can produce geochemical characteristics similar to those ascribed to contributions from the lithospheric mantle.

The aim of our investigation is to contribute to this debate through study of the Rodeo and Nazas volcanic fields in the southern Basin and Range Province of Durango, México. The extensional and magmatic characteristics of this region are not well known. We describe (1) the timing and character of Oligocene–earliest Miocene extension, (2) the petrology and geochemistry of Miocene mafic alkalic volcanic rocks, termed hawaiites, that erupted during the ca. 24 Ma extensional pulse, and (3) the correlation between magma characteristics and the evolving tectonic and thermal state of the lithosphere. We find that megacryst incorporation, crystallization, and crustal interaction seriously complicate attempts to infer mantle-source parameters for these early Basin and Range Province magmas.

MID-CENOZOIC MAGMATIC-TECTONIC SETTING OF THE RODEO-NAZAS AREA

The Rodeo-Nazas area is in the southern Basin and Range Province of Durango, México (Fig. 1). Oligocene–early Miocene faulting in this area constitutes some of the earliest extension in Durango and in this part of the Basin and Range Province (Henry and Aranda-Gómez, 1992; Aguirre-Díaz and McDowell, 1993; Stewart and Roldán-Quintana, 1994; Aranda-Gómez et al., 1997; Gans, 1997). Although it is east of the relatively unextended, central core of the Sierra Madre Occidental, the Rodeo-Nazas area is within the broader region of the mid-Tertiary Sierra Madre Occidental volcanic province (McDowell and Clabaugh, 1979; Aguirre-Díaz and McDowell, 1991). The rocks that crop out over much of the area are rhyolitic ash-flow tuffs and intermediate lavas that were emplaced between ca. 51 and 30 Ma (Aguirre-Díaz and McDowell, 1991; this report). Hawaiitic volcanism that accompanied a major episode of extension beginning ca. 24 Ma is the focus of this paper.

The oldest exposed rocks are Cretaceous limestone and shale that were likely folded during Laramide deformation (Fig. 2). Folded Cretaceous sedimentary rocks crop out extensively around Nazas and throughout north-central México. They form the footwall of the major normal fault (Rodeo fault) along the east side of the Rodeo valley, but pre-Cenozoic rocks are not exposed in the hanging wall to the west. The nearest known pre-Cenozoic outcrop west of the Rodeo fault is in the Gulf of California lowlands, west of the Sierra Madre Occidental, where Cretaceous sedimentary rocks are intruded by Cretaceous to Eocene batholiths (Bonneau, 1970; Henry and Fredrikson, 1987).

Volcano-Tectonic Episodes

Volcanic rocks in the Rodeo-Nazas area formed during two major volcano-tectonic episodes: (1) dominantly silicic and lesser intermediate subduction-related volcanism of the Sierra Madre Occidental between ca. 51 Ma and 30 Ma, and (2) intraplate-type mafic alkalic hawaiites ca. 24 Ma (Aguirre-Díaz and McDowell, 1991, 1993; Aranda-Gómez et al., 1997; this report). Field relations demonstrate that extension began in the area between 32.3 and 30.6 Ma. A second major pulse of extension followed ca. 24 Ma, although minor faulting may have continued intermittently between these times. The older extensional episode was contemporaneous with the youngest Sierra Madre Occidental magmatism in the area. The younger extensional episode was contemporaneous with hawaiite eruptions. Still later episodes of extension, ca. 12 Ma and in Quaternary time, are recognized elsewhere in Durango (Aranda-Gómez and Henry, 1992; Henry and Aranda-Gómez, 1992, 2000; Aranda-Gómez et al., 1997), and may have occurred in the Rodeo-Nazas area.

From K-Ar dating near Nazas, Aguirre-Díaz and McDowell (1991) recognized two episodes of prehawaiitic magmatism between 51

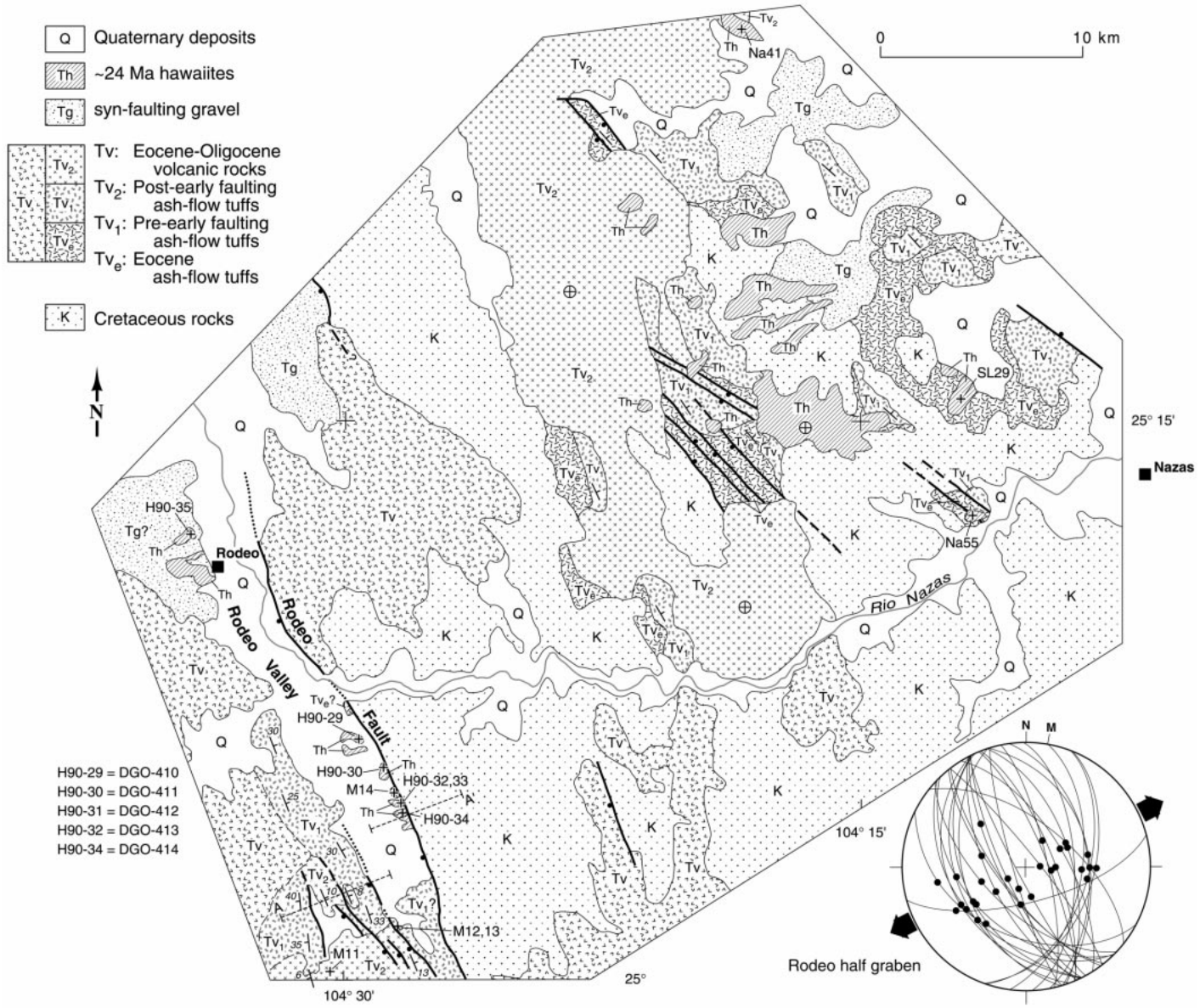

Figure 2. Simplified geologic map of Rodeo-Nazas area (Enciso-De La Vega, 1963; Aguirre-Díaz and McDowell, 1991; our unpublished work). Wulff, lower hemisphere plot shows fault and slickenline data from the Rodeo half graben. Arrows indicate least principal stress (σ_3). Paleostress analysis using the method of Angelier (1979), as well as general fault, graben, and tilt orientations, shows that faulting resulted from east-northeast extension.

and 40 Ma and at 30 Ma. Major rhyolitic tuffs erupted at 51 Ma (Abasolo tuff) and 43 Ma (Boquillas Coloradas tuff), and minor andesitic lavas erupted at 49, 45, and 40 Ma during the first episode. Two voluminous, composite ash-flow tuffs erupted in the second episode. The older Cerro Prieto tuff has a preferred average age of 29.9 ± 1.6 Ma and is faulted and tilted (Aguirre-Díaz and McDowell, 1991). The overlying Santa Clara tuff has a single age of 29.5 ± 0.6 Ma and is flat lying and unfaulted. These and similar rocks near Rodeo are part of the main, Oligocene ignimbrite flare-up of the Sierra Madre Occidental (McDowell and Keizer, 1977; Swanson et al., 1978; McDowell and Clabaugh, 1979).

The prehawaiite volcanic sequence around the Rodeo valley is broadly similar to that of the Nazas area. A rhyolitic tuff, petrographically similar to the Boquillas Coloradas tuff, occurs as a sliver along the Rodeo fault and gives a $^{40}Ar/^{39}Ar$ age of 42.13 ± 0.11 Ma (Table 1). A series of ash-flow tuffs overlies undated andesitic lavas in the hanging wall west of the valley. The andesite and several ash-flow tuffs that directly overlie it are faulted and moderately tilted. These are overlain in angular unconformity by a tuff that is faulted but only gently tilted. The $^{40}Ar/^{39}Ar$ ages are 32.33 ± 0.09 Ma on the stratigraphically highest of the tilted tuffs and 30.62 ± 0.09 Ma on the overlying, less tilted tuff (Table 1). These ages allow possible correlation with tuffs near Nazas; on the basis of petrographic similarities, the younger tuff is probably part of the Santa Clara tuffs. Sources of the tuffs are unknown but definitely not in the immediate vicinity of Rodeo and Nazas.

Hawaiites were emplaced as lavas or shallow

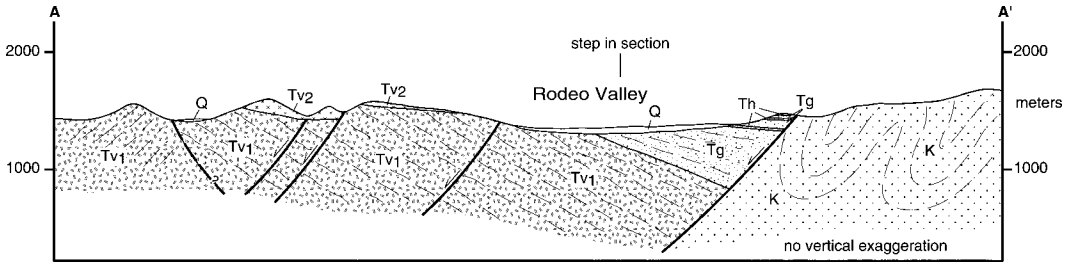

Figure 3. Cross section across Rodeo half graben; cross section is enlarged four times relative to Figure 2, which shows the location. Section is in two parallel, east-northeast–trending segments offset by ~3 km. Eocene–Miocene volcanic rocks were downdropped along the major west-dipping Rodeo fault in two separate episodes or during a continuum of faulting between ca. 30 and 24 Ma. Older Oligocene ash-flow tuffs (Tv_1; ca. 32 Ma) are tilted to the east, commonly as much as 35°, and repeated by several small-displacement, west-dipping faults, but roll over to a westward dip across a poorly understood fault. Younger Oligocene ash-flow tuffs (Tv_2; ca. 30.6 Ma) overlie the older tuffs in an angular unconformity and dip gently eastward. Hawaiites (Th) erupted from vents at least in part along the Rodeo fault ca. 24 Ma and are partly intrusive and partly interbedded with synfaulting gravel (Tg). Fanning dips in gravel are speculative.

intrusions in the Rodeo valley and near Nazas (Fig. 2). In the Rodeo valley, hawaiites crop out in the hanging wall of the Rodeo fault, where they are interbedded with or intrude conglomerates that accumulated in the half graben. The large northern body makes a roughly circular ring in which flow foliation dips radially inward (H90-29 locality). This was probably a ring dike that intruded poorly consolidated sediments. Several hills to the south consist of lavas interbedded with conglomerate. In the southernmost outcrops along the Rodeo fault, two 8-m-thick lava flows are separated and overlain by conglomerate and sandstone. Clasts in the conglomerate are exclusively rhyolites similar to those that crop out to the west. The contact between conglomerate and rhyolite is covered by Quaternary deposits, and the thickness of conglomerate is unknown. The Rodeo fault cuts hawaiites at several locations. All hawaiites contain abundant megacrysts and glomerocrysts of sodic plagioclase, clinopyroxene, olivine, and spinel.

Hawaiites near Nazas crop out in several plateaus as flat-lying lavas, some of which connect to deeply dissected cones (Aguirre-Díaz and McDowell, 1993). The lavas overlie tilted rhyolitic tuffs or flat-lying conglomerates, presumably shed from fault blocks. Aguirre-Díaz and McDowell (1993) recognized several vents along normal faults, but the hawaiites are not faulted.

K-Ar ages on hawaiites from both areas indicate that most were emplaced ca. 24 Ma, but some near Nazas may be as young as 20 Ma (Table 1; Aguirre-Díaz and McDowell, 1993). Four K-Ar ages on plagioclase from Rodeo samples have a narrow range, ca. 24 Ma (Table 1); these ages were confirmed by $^{40}Ar/^{39}Ar$ results completed too late for inclusion in this study. Aguirre-Díaz and McDowell (1993) reported five ages on four hawaiitic samples, three from Nazas and one from Rodeo. A whole-rock age from the ring intrusion yielded 22.4 ± 0.4 Ma, whereas our plagioclase sample from the same body gave 24.1 ± 0.6 Ma. Other whole-rock ages on Nazas hawaiites were 24.3 ± 0.5, 22.1 ± 0.4 (in agreement with a coexisting plagioclase megacryst, 21.2 ± 0.6), and 20.3 ± 0.4 Ma (Aguirre-Díaz and McDowell, 1993). The difference between our age and that of Aguirre-Díaz and McDowell (1993) for the ring intrusion and their lower whole-rock ages suggests either minor Ar loss from whole-rock samples or excess Ar in plagioclase. We favor minor Ar loss because the Rodeo plagioclase ages are so consistent (Table 1). However, the agreement between Aguirre-Díaz and McDowell's whole-rock (22.1 ± 0.4 Ma) and plagioclase (21.2 ± 0.6 Ma) ages on the one sample suggest that emplacement may have occurred over several million years. All analyses were done at the University of Texas at Austin, so interlaboratory bias is not an issue.

TABLE 1. K-Ar AND $^{40}Ar/^{39}Ar$ AGES, RODEO GRABEN

Sample	Mineral	K (%)	Age method	$^{40}Ar^*$ ($\times 10^{-6}$ scc/g)	Ar* (%)	n	Age (Ma)	±1σ	±2σ
K-Ar ages, Hawaiites (Th)									
H90-29A, ring intrusion	Plagioclase	0.524		0.4881	44.8		24.1	0.6	
H90-30b, cut by fault	Plagioclase	0.879		0.8449	63.1		23.8	0.7	
		0.869		0.7815	59.3				
H90-32b, upper lava	Plagioclase	0.443		0.3525	33.8		23.3	3.0	
		0.428		0.4472	33.1				
		0.444							
H90–33, lower lava	Plagioclase	0.634		0.5797	48.8		23.8	0.5	
		0.629		0.5957	49.5				
$^{40}Ar/^{39}Ar$ ages, Ash-flow tuffs									
M-11, Tv_2	Sanidine		Single crystal, mean			15	30.62		0.09
M-13, Tv_2	Sanidine		Single crystal, mean			15	30.62		0.09
	Sanidine		Single crystal, mean			8	30.46		0.13
M-12, Tv_1	Sanidine		Single crystal, mean			11	32.33		0.09
M-14, Tv_e	Sanidine		Single crystal, mean			15	42.13		0.11

Note: n = number of single grains analyzed. Decay constants and isotopic abundances after Steiger and Jäger (1977). Minerals were separated from crushed, sieved samples by standard magnetic and density techniques; concentrates were leached with dilute HF to remove matrix and then handpicked. Complete isotopic data and analytical parameters are presented in Table DR1 (GSA Data Repository; see text footnote 1). K-Ar analytical methods: McDowell (1983) and McDowell and Mauger (1994). 1σ uncertainty for K is ± 1.25% for plagioclase with K concentrations <2%; 1σ uncertainty for Ar is ±2.0% for samples that are more than 30% radiogenic. $^{40}Ar/^{39}Ar$ methods: McIntosh and Chamberlain (1994). Samples were irradiated in Al discs for 7 h in the D-3 position, (Nuclear Science Center, College Station, Texas). Neutron flux monitor Fish Canyon Tuff sanidine (FC-1). Assigned age = 27.84 Ma (Deino and Potts, 1990) relative to Mmhb-1 at 520.4 Ma (Samson and Alexander, 1987). Weighted mean $^{40}Ar/^{39}Ar$ ages calculated by the method of Samson and Alexander (1987).
*Radiogenic.

Geometry and Timing of Extension

The Rodeo valley is a north-northwest–striking half graben at least 25 km long that is bounded on the east by the Rodeo fault, a major, west-dipping normal fault (Figs. 2 and 3). The footwall consists of folded Cretaceous limestone in the south half of the gra-

ben and undated, flat-lying rhyolitic tuffs in the north half. Rocks in the hanging wall include the hawaiites and interbedded conglomerate, the two generations of ash-flow tuffs, and undated andesite that underlies the older tuffs.

Along the western side of the Rodeo valley, the older rhyolitic rocks dip as much as 35° eastward and are repeated by several, southwest-dipping, moderate-displacement normal faults. About 6 km west of the eastern boundary fault and across a zone of north-northwest−striking faults, dip reverses to as much as 40° westward. The 30.6 Ma ash-flow tuff unconformably overlies the older rhyolites and some fault scarps, is cut by younger faults, and is tilted generally no more than 10°. The 24 Ma hawaiites and conglomerates on the eastern side of the valley are flat lying to gently west tilted and locally cut by the Rodeo fault. The contact between the rhyolitic volcanic rocks and the hawaiite-conglomerate sequence is covered by Quaternary alluvium in the valley floor.

All major faults of the Rodeo half graben strike north-northwest and dip 40°−80° southwest; minor faults also dip to the northeast (Fig. 2). Measured dips on the Rodeo fault are 42° and 50°, and the tilt of rocks in the hanging wall suggests that it is listric. Displacement on the Rodeo fault must be at least 3 km to restore the Tertiary rocks above the Cretaceous. Displacement on faults in the hanging wall ranges to ~300 m. The geometries of the faults and the overall half graben suggest that the Rodeo fault is a master or breakaway fault. The dip reversal to the west may be a rollover anticline. Despite this reversal, most tilts near Rodeo and throughout Durango east of the Sierra Madre Occidental are to the east-northeast. This is part of a pattern of east-northeast tilts all along the ~1000 km length of the Sierra Madre Occidental (Stewart et al., 1998).

The north-northwest strike of the half graben and individual faults, the direction of stratal tilt, and paleostress analysis of 31 measured faults and slickenlines using the method of Angelier (1979) indicate east-northeast extension (Fig. 2). The total amount of extension is unknown, but large enough to generate stratal tilts of as much as 40°.

These relations indicate two episodes or, less likely, a 6 m.y. continuum of faulting. The angular unconformity between the two tuff sequences demonstrates a major episode of faulting and tilting between 32.3 and 30.6 Ma. The greatest amount of extension probably occurred in this episode, because the 30.6 Ma rocks are much less tilted. The second episode occurred ca. 24 Ma, contemporaneous with hawaiite eruptions. Hawaiites are interbedded with conglomerates that filled the Rodeo half graben and are cut by the Rodeo fault. Displacement of hawaiites and conglomerates by the fault and the lack of Cretaceous clasts in the conglomerates indicate that these rocks did not simply fill a graben that formed before 30.6 Ma and became inactive.

The style and timing of faulting in the Nazas area are similar to those at Rodeo (Aguirre-Díaz and McDowell, 1993). Faults strike northwest and mostly dip to the southwest; maximum displacement is ~300 m. Fault orientations and sparse slickenline data imply northeast extension. Volcanic units ca. 30 Ma and older are faulted and irregularly tilted. Cross sections in Aguirre-Díaz and McDowell (1993) show dominantly northeast dips, to as much as 35°, but also show abrupt transitions to approximately flat-lying rocks and, in one case, to a southwest dip, possibly another rollover anticline. Volcanic and sedimentary rocks ca. 30 Ma and younger are untilted and apparently unfaulted. The less precise K-Ar ages indicate that faulting and tilting occurred ca. 30 Ma.

Extension at Nazas is different than at Rodeo in two significant ways. First, hawaiites and underlying fanglomerates are not faulted at Nazas, which may indicate that faulting ceased before ca. 24 Ma. Alternatively, hawaiites near Nazas may be younger than those near Rodeo and simply postdate the 24 Ma episode of faulting. Second, total extension at Nazas is probably less than at Rodeo. All faults near Nazas have modest displacements, similar to the hanging-wall faults of the Rodeo half graben. Cretaceous basement rocks are widely exposed. A distinct, conglomerate-filled half graben and major breakaway fault as in the Rodeo valley are not present at Nazas. Such a graben and major fault may be present ~10 km east of Nazas, where a regional geologic map shows a broad valley bounded on the east by ridges of folded Cretaceous rocks (Instituto Nacional de Estadistica Geografia e Informatica, 1988). This is physiographically similar to the Rodeo valley, but the map does not depict any structure.

Oligocene extension in the Rodeo-Nazas area is the earliest recognized episode in the southern Basin and Range Province. In contrast, late Oligocene−earliest Miocene extension (ca. 27–22 Ma) has been recognized in several areas, and includes mostly high-angle faulting and moderate total extension in Sonora (Stewart and Roldán-Quintana, 1994; Bartolini et al., 1995; Gans, 1997; McDowell et al., 1997), the Salton trough (Kerr and Kidwell, 1991), southwestern Arizona (Spencer et al., 1995), north of Guadalajara at the southern end of the Sierra Madre Occidental (Moore et al., 1994; Nieto-Samaniego et al., 1999), and Texas (Henry and Price, 1986; Henry et al., 1991), and detachment faulting and core-complex development in Arizona and Sonora (Spencer and Reynolds, 1989; Nourse et al., 1994; Spencer et al., 1995). Note that high-angle faulting and moderate extension, detachment faulting, core-complex development, and high-magnitude extension were occurring in adjacent parts of Arizona and Sonora at the same time. Presumably these are different manifestations of the same extensional episode. The characteristics of extension and accompanying magmatism in the Rodeo-Nazas area are most similar to those in Texas. Initial basin and range faulting in Texas began ca. 24 Ma, produced a series of north-northwest−striking half graben, and was accompanied by megacrystic hawaiites that are petrographically and compositionally indistinguishable from those at Rodeo and Nazas.

PETROLOGY AND GEOCHEMISTRY

Petrography and Mineralogy

Hawaiites from the Rodeo-Nazas area have many characteristics in common with volcanic rocks from other intraplate-type Miocene volcanic fields in the southern Basin and Range Province: the 24–17 Ma Trans-Pecos field of west Texas (James and Henry, 1991, 1993), the 11–14 Ma Los Encinos field of San Luis Potosí and Zacatecas (Luhr et al., 1995b), and the 12 Ma Metates lava flows of Durango (McDowell and Keizer, 1977; Swanson et al., 1978; Smith, 1989; Aranda-Gómez et al., 1997). Specifically, these suites (1) are dominated by moderately evolved, intraplate-type (high Ti, Nb, Ta) mafic alkalic rocks, classified as hawaiites, (2) commonly carry abundant megacrysts, and (3) are typically free of granulitic or peridotitic xenoliths, with the exception of rare peridotite xenoliths from the Trans-Pecos area (Nelson and Schieffer, 1990; James and Henry, 1993) and occasional small feldspathic granulite xenoliths at Los Encinos (Luhr et al., 1995b).

Point-counted modes for the nine studied Rodeo-Nazas rocks are listed in Table DR2 (GSA Data Repository[1]). The stable minerals

[1]GSA Data Repository item 2001060, $^{40}Ar/^{39}Ar$ results and mineralogy, is available on the Web at http://www.geosociety.org/pubs/ft2001.htm. Requests may also be sent to Documents Secretary, GSA, P.O. Box 9140, Boulder, CO 80301; e-mail: editing@geosociety.org.

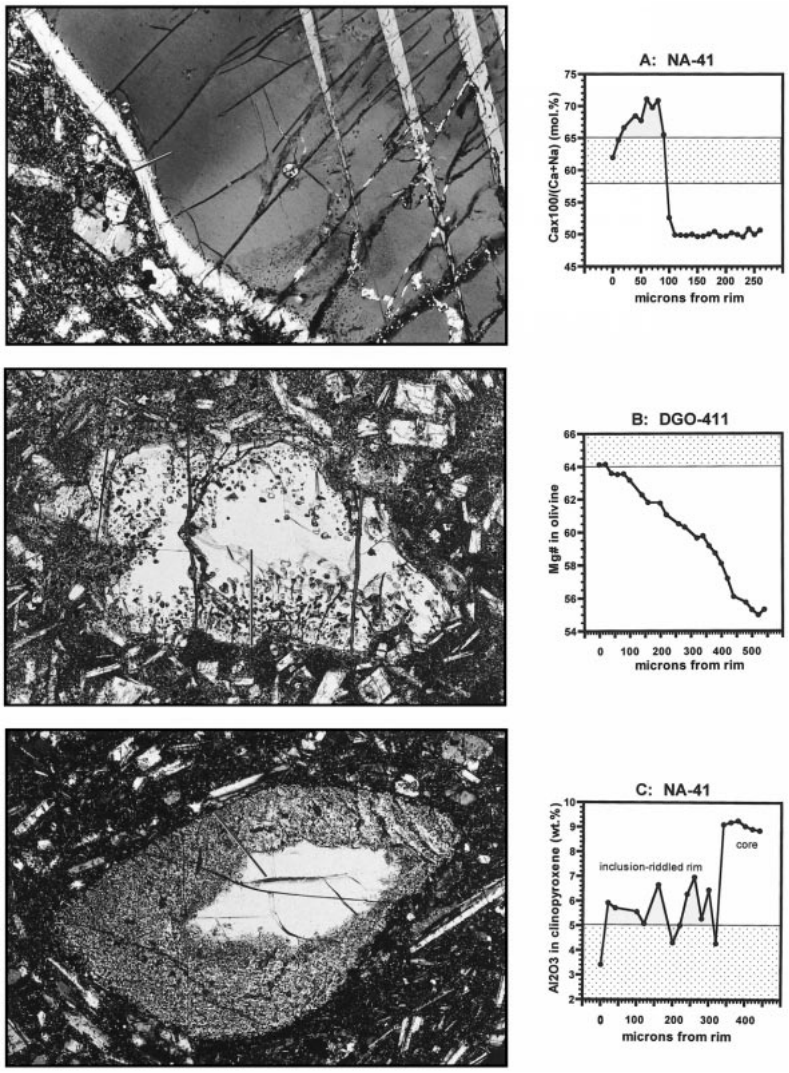

Figure 4. Photomicrographs (2.8 mm across) of megacrysts in Rodeo-Nazas samples. Black and white lines show positions of accompanying compositional profiles. Stippled fields indicate the compositional ranges for homogeneous phenocrysts and microphenocrysts of plagioclase ($An_{57–65}$), olivine ($Fo_{64–69}$), and clinopyroxene (1–5 wt% Al_2O_3). (A) Sodic plagioclase megacryst in sample NA-41 with 100 μm reaction rim of stable calcic plagioclase, in cross-polarized light. (B) Fe-rich olivine megacryst in sample DGO-411 with glass-inclusion−riddled reaction rim, in plane light. (C) Al-rich clinopyroxene megacryst core in sample NA-41 surrounded by glass-inclusion−riddled rim that is relatively poor in Al, in plane light.

in all Rodeo-Nazas rocks include phenocrysts (>0.3 mm across) of plagioclase and olivine, and microphenocrysts (0.03–0.3 mm across) of the same phases plus clinopyroxene and titanomagnetite. Four of the samples also have microphenocrysts of biotite. Most Rodeo-Nazas hawaiites also contain centimeter-sized megacrysts of sodic feldspar (Fig. 4A), Fe-rich olivine (Fig. 4B), Al-rich clinopyroxene (Fig. 4C), and a compositionally wide variety of individually homogeneous spinels. Each of these megacryst types has an abrupt overgrowth rim similar in composition to the rims of stable phenocrystic and microphenocrystic minerals. Representative electron microprobe analyses of stable and megacrystic minerals are listed in Tables DR3−DR6 (see footnote 1).

Slight to strong alteration has affected the Rodeo-Nazas hawaiites. Slight alteration involves conversion of olivine rims to iddingsite. More advanced alteration includes nearly complete iddingsite replacement of olivine microphenocrysts and phenocryst rims, patchy conversion of glass, olivine, and plagioclase to smectite, zeolites, chlorite, and calcite, oxidation and exsolution of titanomagnetite and ferrian ilmenite, and filling of vesicles by zeolites and calcite. Among the stable minerals, only clinopyroxene appears to be unaffected by alteration.

Relatively homogeneous plagioclase microphenocrysts and phenocrysts to 350 μm across have compositions of $An_{57–65}$. Larger plagioclase crystals (megacrysts) typically have approximately homogeneous sodic cores that vary from crystal to crystal between An_{26} and An_{51} (Fig. 4A). These sodic cores are abruptly surrounded by normally zoned, more calcic rims similar in composition to the phenocrysts. Some of the plagioclase megacryst cores include or abut other phases, giving evidence of phase assemblages prior to megacryst disaggregation. In sample DGO-411, two sodic plagioclase megacryst cores ($An_{27–32}$) have apatite, spinel, and smaller pyrrhotite crystals as inclusions. Other plagioclase megacrysts are intergrown with megacrysts of spinel, clinopyroxene, or symplectite-like aggregates of fine clinopyroxene + olivine. Some of the sodic plagioclase megacrysts associated with these other phases lack prominent calcic overgrowths.

Most olivine phenocrysts show normal zoning with rims of $Fo_{64–69}$ and cores as magnesian as Fo_{80}. The larger (megacrystic) olivine crystals have glass-inclusion−riddled margins and are reversely zoned (Fig. 4B). Approximately homogeneous cores of Fo_{55} transition outward to more Mg-rich compositions through the glass-inclusion-riddled zone, reaching rims similar to those of phenocrysts at $Fo_{64–66}$.

Two distinct clinopyroxene compositional populations are present in every sample. Phenocrysts, microphenocrysts, and groundmass crystals have compositions that broadly cluster about $Fe_{14}Mg_{41}Ca_{45}$, with 1–5 wt% Al_2O_3. In contrast, the compositionally homogeneous cores of megacrysts are roughly similar to the first type in their proportions of Fe:Mg:Ca, but have about twice the Al contents at 7–9 wt% Al_2O_3 (Fig. 4C). These Al-rich megacryst cores are typical of clinopyroxene megacrysts and pyroxenite xenoliths associated with intraplate-type mafic alkalic volcanic rocks throughout the world, designated the Al-augite group by Wilshire and Shervais (1975). The Al-rich clinopyroxene megacryst cores in Rodeo-Nazas hawaiites are surrounded by glass-inclusion−riddled margins with Al-poor clinopyroxene compositions, some similar to the stable microphenocrysts (Fig. 4C). These in-

clusion-riddled zones vary widely in thickness (20–340 μm).

Titanomagnetites with 17–25 wt% TiO_2 are present as microphenocrysts and ubiquitous as groundmass crystals in all samples. Other tiny spinels are included within olivine microphenocrysts and phenocrysts. Some are compositionally similar to isolated titanomagnetites, whereas others are rich in Al, Cr, and Mg. Spinel crystals larger than 0.3 mm (megacrysts) have compositions that are quite distinct from the stable titanomagnetites, generally being poorer in TiO_2, FeO^{total}, and MnO, and richer in Al_2O_3, Cr_2O_3, MgO, and NiO. Some of these are intergrown with or included within megacrysts of other minerals, and those adjacent to groundmass are typically surrounded by a rim of titanomagnetite.

Whole-Rock Geochemistry

Nine Rodeo-Nazas samples were analyzed for major and trace elements by X-ray fluorescence (XRF) spectroscopy and instrumental neutron activation (INA) (Table 2). Six of these samples were also analyzed for Sr, Nd, and Pb isotopic ratios (Table 3). In the following sections we discuss the geochemistry of the Rodeo-Nazas suite in relation to data for other Miocene hawaiites from the Mexican Basin and Range Province.

The Rodeo-Nazas samples have the elevated abundances of TiO_2 (2.1–2.4 wt%), Nb (40–82 ppm), and Ta (2.1–4.2 ppm) that characterize intraplate-type mafic volcanic suites worldwide. They are classified as hawaiites based on the total alkali-silica diagram of the International Union of Geological Sciences system (Le Bas et al., 1986). Eight of the nine samples have normative Ne (1.1–3.8 wt%); sample H90–35 contains 5.0 wt% normative Hy, which might be a consequence of alteration because this sample contains both strongly altered olivine and ~15 vol% coarse patches of smectite and chlorite (Table DR2; see footnote 1). However, it is common for intraplate-type volcanic suites of the Mexican Basin and Range Province to have a small percentage of Hy-normative samples, which show no clear relationship to extent of alteration.

Compared to other Miocene hawaiites of the Mexican Basin and Range Province, those from Rodeo and Nazas are typical with respect to MgO (5.5–7.1 wt%), Mg# (52.2–59.7), Ni (48–83 ppm), and Cr (73–186 ppm). These parameters all signify that the Rodeo-Nazas hawaiites are differentiated and could not have originated by direct partial melting of peridotitic mantle.

TABLE 2. WHOLE-ROCK MAJOR AND TRACE ELEMENT ANALYSES

Field	Rodeo	Rodeo	Rodeo	Rodeo	Rodeo	Rodeo	Nazas	Nazas	Nazas
Sample	DGO-410	DGO-411	DGO-412	DGO-413	DGO-414	H90-35	NA-55	SL-29	NA-41
Lat (°N)	25.1084	25.0957	25.0919	25.0797	25.0750	25.1937	25.2106	25.2589	25.4256
Long (°W)	104.4908	104.4821	104.4824	104.4768	104.4737	104.5671	104.1931	104.2006	104.3019
Major elements by XRF (wt%)*									
SiO_2	48.82	49.45	48.63	47.36	48.73	49.38	49.11	48.97	48.06
TiO_2	2.42	2.24	2.40	2.01	2.32	2.32	2.36	2.17	2.26
Al_2O_3	16.51	16.94	16.13	16.55	16.28	16.46	16.80	16.44	16.78
Fe_2O_3	2.46	2.54	5.61	5.46	4.26	2.31	3.95	5.47	2.35
FeO	8.21	8.14	5.54	4.61	6.34	7.99	6.50	5.52	7.94
MnO	0.18	0.19	0.18	0.16	0.17	0.18	0.17	0.18	0.17
MgO	6.35	5.43	5.93	6.60	5.97	6.50	6.09	5.46	7.09
CaO	7.96	7.25	7.88	9.57	7.73	8.29	8.40	7.08	8.58
Na_2O	4.04	5.00	4.07	3.16	3.90	3.31	3.72	4.06	3.85
K_2O	1.93	1.22	1.63	1.69	1.77	1.77	1.77	2.18	1.74
P_2O_5	0.66	0.75	0.78	0.47	0.70	0.62	0.47	0.55	0.65
LOI	0.60	0.62	1.14	2.13	1.59	0.90	0.62	2.03	0.64
Total	100.14	99.75	99.92	99.77	99.76	100.03	99.94	100.11	100.10
Mg#†	56.09	52.21	54.01	59.24	55.17	57.52	55.93	52.30	59.65
CIPW Norm (wt%)†									
or	11.46	7.27	9.81	10.28	10.70	10.58	10.58	13.18	10.34
ab	27.72	35.64	31.43	22.98	31.55	28.26	28.69	30.44	24.67
an	21.34	20.41	21.24	26.72	22.17	25.07	24.13	20.66	23.52
ne	3.59	3.80	1.95	2.45	1.15	0.00	1.65	2.58	4.38
di	11.48	9.06	10.94	15.47	10.11	10.08	12.16	9.58	12.26
hy	0.00	0.00	0.00	0.00	0.00	5.04	0.00	0.00	0.00
ol	15.72	15.26	15.57	14.70	15.66	12.63	14.72	15.46	16.56
mt	2.54	2.54	2.60	2.36	2.51	2.45	2.45	2.58	2.45
ilm	4.62	4.29	4.63	3.93	4.50	4.44	4.52	4.22	4.31
ap	1.53	1.74	1.83	1.11	1.64	1.46	1.09	1.30	1.51
Trace elements by XRF (ppm)§									
V	213	168	200	188	193	210	247	160	217
Ni	68	50	58	60	59	64	49	48	83
Cu	34	27	35	46	46	27	28	30	34
Zn	85	83	88	80	81	86	88	73	83
Rb	36	10	20	35	34	35	35	53	42
Sr	682	674	663	691	687	556	663	571	610
Y	34	35	36	33	33	32	29	32	29
Zr	263	272	265	276	267	195	208	249	200
Nb	63	82	66	68	67	48	40	70	45
Ba	606	674	635	634	632	592	590	718	724
Trace elements by INA (Na_2O and FeO as wt%, others as ppm)#									
Na_2O	4.01	4.95	4.09	3.23	3.85	3.25	3.74	4.21	3.97
FeO	10.35	10.38	10.54	9.49	10.06	9.82	9.96	10.25	10.3
Sc	23.3	19.3	21.4	23.3	21.7	23.6	22.1	19.3	25.6
Cr	110	89	91	136	103	142	73	102	186
Co	37.2	32.4	35.5	37.4	34.6	35.3	36.7	33.0	39.9
Cs	12.6	109.9	11.4	1.29	26.3	2.97	0.84	2.6	3.01
La	34.5	42.2	37.2	32.6	36.8	29.3	28.0	37.0	26.8
Ce	67.5	79.7	71.9	62.7	71.6	58.6	56.4	70.0	54.9
Nd	36	36	38	24	30	27	31	31	27
Sm	6.81	7.30	7.21	5.57	6.91	6.49	6.05	6.43	6.18
Eu	2.24	2.38	2.38	1.88	2.26	2.05	1.96	2.08	2.02
Tb	0.97	1.00	1.00	0.76	0.96	0.93	0.81	0.89	0.89
Yb	2.78	3.05	2.91	2.37	2.88	2.72	2.33	2.68	2.49
Lu	0.41	0.44	0.42	0.34	0.42	0.41	0.35	0.41	0.38
Hf	5.19	5.54	5.27	3.90	5.41	4.36	4.58	5.66	4.67
Ta	3.29	4.20	3.45	3.03	3.67	2.66	2.37	3.79	2.16
Th	4.43	5.51	4.47	3.87	4.83	3.55	2.97	5.22	3.27
U	1.20	2.10	1.40	1.06	1.50	1.13	0.86	1.77	0.98

*XRF (X-ray fluorescence) analyses were performed on the Smithsonian's Philips PW 1480 spectrometer. Major elements were determined on glass disks prepared from 9:1 mixtures of Li-tetraborate and rock powder that had been heated and oxidized during loss on ignition (LOI) determination. Precisions (1σ) were estimated by repeated analysis of one sample and correspond to the following values: SiO_2 = 0.26 wt%, TiO_2 = 0.02%, Al_2O_3 = 0.09%, $Fe_2O_3^{Total}$ = 0.22%, MnO = 0.01%, MgO = 0.08%, CaO = 0.02%, Na_2O = 0.06%, K_2O = 0.04%, and P_2O_5 = 0.01%. FeO was determined by K-dichromate titration following a modified version of the method of Peck (1964). Fe_2O_3 was then calculated from the XRF value for total iron. LOI values are measurements at 1000 °C for 1 h on powders dried for several hours at 110 °C. These LOI values have not been corrected for oxygen uptake upon conversion of FeO to Fe_2O_3 in the furnace.

†Mg# [magnesium number = 100 × Mg/(Mg + Fe^{2+})] and CIPW norms were calculated assuming Fe^{2+} = 0.85 × Fe^t. CIPW norms are on a recalculated anhydrous basis.

§Trace element analyses by XRF were determined at the Smithsonian on pressed disks made from mixtures of 1.6 g rock powder and 0.4 g cellulose, with a boric acid backing. Precisions (1σ) were estimated by repeated analysis of one sample and correspond to the following percentages of the amounts present: V (19), Ni (4), Cu (8), Zn (2), Rb (3), Sr (1), Y (6), Zr (2), Nb (6), Ba (2).

#Trace element analyses by INA (instrumental neutron activation) were performed at Washington University (Lindstrom and Korotev, 1982; Korotev, 1996). Estimated counting errors (1σ) correspond to the following percentages of the amounts present: Na_2O (1.6), FeO (1.3), Sc (1.3), Cr (1.4), Co (1.3), Cs (2.6), La (1.3), Ce (1.3), Nd (12.9), Sm (1.5), Eu (1.9), Tb (2.6), Yb (2.1), Lu (3.7), Hf (2.1), Ta (2.7), Th (1.8), and U (14.4).

TABLE 3. Sr, Nd, AND Pb ISOTOPIC DATA FOR RODEO-NAZAS SAMPLES

Field	Rodeo	Rodeo	Rodeo	Nazas	Nazas	Nazas
Sample	DG0-410	DGO-411	DGO-413	NA-55	SL-29	NA-41
As measured						
$^{87}Sr/^{86}Sr$*	0.703896	0.703751	0.703705	0.704148	0.704118	0.704158
$^{143}Nd/^{144}Nd$†	0.512841	0.512863	0.512876	0.512768	0.512772	0.512809
ϵ_{Nd}	4.0	4.4	4.6	2.5	2.6	3.3
$^{206}Pb/^{204}Pb$§	18.9770	18.9518	18.9393	18.8845	18.8768	18.8202
$^{207}Pb/^{204}Pb$	15.6030	15.5938	15.5949	15.5830	15.5750	15.6003
$^{208}Pb/^{204}Pb$	38.6970	38.6483	38.6917	38.6228	38.6006	38.6088
Pb (ppm)#	3.90	4.10	3.09	4.12	4.09	4.72
Corrected to 24 Ma						
$^{87}Sr/^{86}Sr$	0.703844	0.703737	0.703655	0.704096	0.704027	0.704090
$^{143}Nd/^{144}Nd$	0.512823	0.512844	0.512854	0.512749	0.512752	0.512787
ϵ_{Nd}	4.2	4.6	4.8	2.8	2.8	3.5
$^{206}Pb/^{204}Pb$	18.9072	18.8356	18.8616	18.8372	18.7787	18.7731
$^{207}Pb/^{204}Pb$	15.5998	15.5884	15.5913	15.5808	15.5705	15.5981
$^{208}Pb/^{204}Pb$	38.6123	38.5481	38.5982	38.5691	38.5053	38.5571

Note: Isotopic analyses were performed on the Finnigan MAT 261 mass spectrometer at the University of Texas at Austin.

*Sr was loaded with H_3PO_4 onto a Ta filament and the isotopic composition was measured in static multicollection mode. Sr isotopic compositions were corrected for mass fractionation using an exponential fractionation law, normalized to $^{86}Sr/^{88}Sr = 0.1194$, and adjusted to NIST SRM-987 = 0.710250. On the basis of the long-term reproducibility of the standard and samples, uncertainties for the Sr isotopic analyses are estimated to be ~0.000020 (2σ).

†Nd was loaded with H_3PO_4 onto a Re side filament of a double-filament assembly, and the isotopic composition was measured in dynamic multicollection mode. Nd isotopic compositions were corrected for mass fractionation using an exponential fractionation law and normalizing to $^{146}Nd/^{144}Nd = 0.7219$. The mean value for long-term analyses of an Ames metal Nd standard used in this lab is $^{143}Nd/^{144}Nd = 0.512089 \pm 11$ (2σ), $\epsilon_{Nd} = -10.70 \pm 0.21$. This corresponds to a value for the CIT nNdβ standard of $^{143}Nd/^{144}Nd = 0.511907$, $\epsilon_{Nd} = -14.25$. On the basis of the long-term reproducibilities of the Ames and CIT nNdβ standards, the estimated uncertainty for a given analysis is ~0.000011 (2σ), corresponding to approximately 0.25 ϵ_{Nd} units. The following model parameters were used: $^{143}Nd/^{144}Nd(CHUR) = 0.512638$; $^{147}Sm/^{144}Nd(CHUR) = 0.1967$.

§Pb was loaded with silica gel and H_3PO_4 onto a Re filament and the isotopic composition was measured in static multicollection mode. The measured Pb isotopic compositions have been corrected for $\alpha = 0.09\%$ a.m.u.$^{-1}$ based upon multiple analyses of NIST SRM-981. Uncertainties for the Pb isotopic compositions are estimated to be 0.05% a.m.u.$^{-1}$ (2σ).

#Pb concentrations were determined by isotope dilution mass spectrometry.

Rodeo-Nazas hawaiites also have typical abundances of most incompatible elements compared to other intraplate-type Miocene−Quaternary volcanic rocks from the Mexican Basin and Range Province. Multielement spider diagrams of six representative Rodeo-Nazas hawaiites are shown in Figure 5A. Their patterns mostly mimic those for nearby Quaternary volcanic rocks (stippled field), with the exception of the two most incompatible elements at the left end of the diagrams: Cs shows exceptional enrichments in four Rodeo hawaiites (11.4–109.9 ppm), and Rb shows a marked depletion in the most Cs-enriched of these (DGO-411).

Many workers have documented the incorporation of Cs into oceanic basalts during hydrothermal alteration (Hart, 1969; Berger et al., 1988; Jochum and Verma, 1996), where Cs concentrations can be increased by factors of 20. Thus, it is logical to consider that the elevated Cs contents in Rodeo hawaiites might be a result of posteruption hydrothermal or surficial alteration. In an attempt to understand where Cs resides in these Rodeo hawaiites, we conducted a series of leaching experiments (Table 4). Two Cs-rich Rodeo samples and a fresh Mexican andesitic lava erupted in 1999 were each leached three different ways: 1N ammonium acetate, 0.1N HCl, and distilled water (Table 4). Ammonium acetate is a cation-exchange reagent used in soil and clay research to release loosely bound, easily exchangeable cations (Morton and Long, 1980; Morton, 1985). The HCl leach is a more aggressive attack on glass and weaker minerals, likely including trace element−rich apatite. Leaching in ammonium acetate resulted in 17%–22% loss of Rb compared to distilled water, but virtually no loss of Cs. Leaching in HCl resulted in 25%–27% loss of Rb, 14%–34% loss of Cs, 24%–39% loss of La, and 24%–40% loss of Ce. These experiments indicate that Rb is more loosely bound than Cs in the Rodeo hawaiites, and that Cs is held about as tightly as La and Ce. These results do not support the notion that Cs was enriched by hydrothermal or surficial alteration following eruption. Consistent with this interpretation is the fact that the most Cs-rich sample, DGO-411, has only slight alteration, with minor marginal smectite rims on olivine (Table DR2; see footnote 1). Many other samples with much lower Cs contents show the petrographic effects of significantly greater alteration.

Multielement spider diagrams for representative samples from other Miocene hawaiite suites from the Mexican Basin and Range Province are shown in Figure 5B. Some samples from Los Encinos also show Cs enrichments (to 6.5 ppm), but their patterns for other elements are distinct from the much more highly Cs-enriched samples from Rodeo, being accompanied by enrichments in Rb, Th, U, and K. It is important to note that other samples from Nazas, Rodeo, Los Encinos, and Metates have patterns similar to the Quaternary samples (Fig. 5, A and B, stippled fields), without any unusual behavior of Cs, Rb, or other elements.

The relationships among Cs, Rb, and Th are emphasized in Figure 6. The low Cs values that characterize all Quaternary samples (0–2 ppm; stippled fields) are shared among Miocene hawaiites by two of the nine Rodeo-Nazas samples, by half of the Los Encinos samples, and by the only analyzed Metates sample. Both Rodeo and Los Encinos hawaiites display correlation trends between Cs and Th (Fig. 6A), but the slopes are dramatically different; Rodeo samples show extremely low Th/Cs, and Los Encinos samples show extremely high Th/Cs, with Th values that greatly exceed any in the Quaternary data set. The plot of Cs versus Rb (Fig. 6B) mimics that for Th, with the exception that the Cs-Rb correlation for Rodeo samples is crudely negative.

Rodeo and Nazas hawaiites have distinct Sr, Nd, and Pb isotopic compositions, although the variations are small (Table 3; Figs. 7 and 8). Relative to Nazas samples, Rodeo hawaiites have lower $^{87}Sr/^{86}Sr_i$ (0.7037–0.7038 vs. 0.7040–0.7041), higher $\epsilon_{Nd,i}$ (4.2–4.8 vs. 2.8–3.5), higher $^{206}Pb/^{204}Pb_i$ (18.84–18.91 vs. 18.77–18.84), and higher $^{208}Pb/^{204}Pb_i$ (38.55–38.61 vs. 38.51–38.57). The $^{207}Pb/^{204}Pb_i$ values overlap (15.57–15.60).

DISCUSSION

Interpretation of Mineralogy and Textures: Origin of the Megacrysts

The relatively evolved compositions of the stable minerals in the Rodeo-Nazas hawaiites, particularly the $An_{57–65}$ plagioclase and $Fo_{64–80}$ olivine, are consistent with the nonprimitive whole-rock MgO, Ni, and Cr values. Megacrysts of plagioclase ($An_{26–51}$), olivine (Fo_{55}), clinopyroxene (7–9 wt% Al_2O_3), and spinel are prominent in most Rodeo-Nazas hawaiites, as they are in other Miocene hawaiites of the southern Basin and Range Province. The megacrysts are as large as 6 cm and homogeneous in composition, except for rims of variable thickness that closely

match compositions for the rims of phenocrysts and microphenocrysts. These megacrysts probably crystallized in a deep plutonic setting, perhaps as bodies of gabbro, from earlier intraplate-type magmas that were similar to the Rodeo-Nazas hawaiites but even more differentiated. That Rodeo-Nazas hawaiites do not contain peridotite xenoliths or xenocrysts implies that these gabbroic bodies were probably located within the crust.

As the Rodeo-Nazas hawaiites later ascended through the same region, they apparently intersected and disrupted these deep-crustal gabbroic plutons, parts of which were carried toward the surface as disaggregating xenoliths. During ascent, individual megacrysts developed overgrowth rims as they attempted to equilibrate with the enclosing melt. The variable thicknesses of reaction rims (10–500 μm) are evidence of the gradual xenolith disaggregation process, as different gabbroic crystals were shed into the melt at different stages of the ascent path. The reaction rim thicknesses reflect the time between contact with the melt and eruptive quenching.

Similar megacryst assemblages are present in the early Miocene (ca. 24 Ma) Trans-Pecos hawaiites and in the middle Miocene (ca. 14–11 Ma) hawaiites from Los Encinos and Metates. To a significantly lesser extent they are also present in some Quaternary suites from the southern Basin and Range Province, especially in the Durango Volcanic Field and at the Punta Piaxtla vent along the Gulf of California coast north of Mazatlan (Smith, 1989).

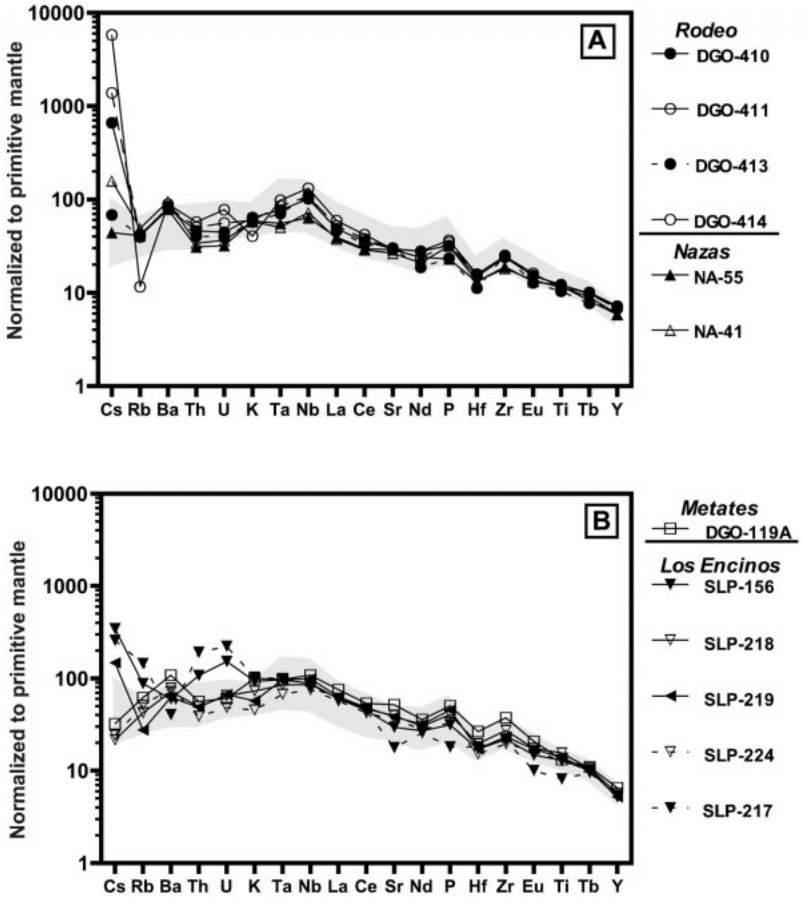

Figure 5. Whole-rock multielement spider diagrams normalized to estimated primordial mantle abundances (after Wood et al., 1981). The stippled fields show the ranges for 50 Quaternary intraplate-type volcanic rocks (hawaiites, alkali basalts, basanites, and olivine nephelinites) from the Mexican Basin and Range Province: the Ventura and Santo Domingo volcanic fields (Luhr et al., 1989), and La Breña–El Jagüey maar complex in the Durango volcanic field (Pier et al., 1992). (A) Six representative samples from the Rodeo and Nazas volcanic fields. (B) Six representative samples from other Miocene volcanic fields in the Mexican Basin and Range Province: Metates (Smith, 1989) and Los Encinos (Luhr et al., 1995b).

Sr, Nd, and Pb Isotopic Evidence for Crustal Contamination

Rodeo samples fall at the enriched end (high $^{87}Sr/^{86}Sr$, low ϵ_{Nd}) of the field for mafic rocks from the Miocene–Quaternary Mexican Basin and Range Province, and the Nazas samples extend that field even farther (Fig. 7), coinciding with data for the subduction-related Mexican Volcanic Belt. Three vectors are shown in Figure 7, indicating documented crustal-contamination trends in mafic magmatic systems from México: two crustal-contamination trends identified in the Los Encinos suite (LEA and LEB; Luhr et al., 1995b), and the classic crustal-contamination trend for the Parícutin suite from the Mexican Volcanic Belt (Par; McBirney et al., 1987; Housh, unpublished data). The Rodeo samples are near the enriched ends of the Los Encinos contamination vectors, and near the least-contaminated end of the Parícutin vector. The Nazas samples, in contrast, are beyond the Los Encinos vectors, near the most contaminated of the Parícutin samples. The two samples with the highest $^{87}Sr/^{86}Sr$ and lowest ϵ_{Nd} from the Rodeo (DGO-410) and Nazas (NA-55) suites are also characterized by the presence of small amounts of quartz xenocrysts or its reaction products (Table DR2; see footnote 1). The most obvious interpretation is that the enriched Sr and Nd isotopic compositions of the Miocene hawaiites from Rodeo, Nazas, and Metates, and the most enriched Quaternary Basin and Range Province samples, have also been affected by crustal contamination.

Pb isotopic ratios of Rodeo-Nazas samples vary slightly, and all are within the field of Quaternary intraplate-type magmas of the Basin and Range Province (Fig. 8A). Virtually all of the volcanic rocks from the Mexican Basin and Range Province and the Mexican Volcanic Belt are above the Northern Hemisphere Reference Line (Hart, 1984), which indicates involvement of one or more additional components besides normal suboceanic mantle. Two possibilities are likely; subcontinental lithospheric mantle and continental crust. The Quaternary samples, most of which are interpreted as having undergone minimal crustal contamination, span a considerable Pb isotopic range, which is likely due to mantle variability. In the same way, the minor Pb isotopic differences between the Rodeo and Nazas hawaiites may simply reflect slight variability in their mantle sources.

Alternatively, the Pb isotopic differences between Rodeo and Nazas hawaiites may reflect crustal contamination of mantle-derived magmas. Evaluation of this possibility is ham-

TABLE 4. TRACE ELEMENT DATA FOR LEACHED POWDERS BY ICP-MS

	Rb	Cs	La	Ce
DGO-411				
XRF/INA*	10.0	109.9	42.2	79.7
DW†	10.1	109.9	41.9	74.4
AA§	8.4	107.6	42.3	75.0
HCl#	7.6	72.4	25.5	44.8
DGO-414				
XRF/INA*	34.0	26.3	36.8	71.6
DW†	31.6	27.4	37.8	68.6
AA§	24.7	27.3	38.5	69.6
HCl#	23.1	23.7	28.6	52.2
COL-99A				
DW†	18.6	0.69	11.3	23.3
AA§	18.6	0.97	11.7	24.0
HCl#	18.2	0.68	9.9	20.0

Note: ICP-MS (inductively coupled plasma-mass spectroscopy) analyses were performed at Washington State University. All measurements are in ppm. Estimated 1σ precisions based on 55 analyses of sample BCR-P correspond to the following percentages of the amounts present: Rb (1.4), Cs (3.1), La (1.9), and Ce (1.2). Leaching experiments on Rodeo hawaiites DGO-411 and DGO-414 were conducted on the same powders used for XRF (X-ray fluorescence) and INA (instrumental neutron activation) analyses (see Table 2). An andesitic lava erupted in 1999 from Volcán Colima, México (COL-99A), was used as a control against the influence of alteration.

*XRF/INA repeats the values listed in Table 2 for comparison.

†DW designates control leaching experiments using 3 g of powder in distilled water for 1 h. The solution and residue were rinsed into filter paper using distilled water, followed by a final acetone rinse. The dried powder was analyzed by ICP-MS.

§AA designates 24 h leaching experiments using 3 g of powder in 50 ml of 1N ammonium acetate, with a mild sonication for 15 min near the middle of the experiment. The solution and residue were rinsed into filter paper using distilled water, followed by a final acetone rinse. The dried powder was analyzed by ICP-MS.

#HCl designates 3 h leaching experiments using 3 g of powder in 50 ml of 0.1N HCl, with a mild sonication for 15 min near the middle of the experiment. The solution and residue were rinsed into filter paper using distilled water, followed by a final acetone rinse. The dried powder was analyzed by ICP-MS.

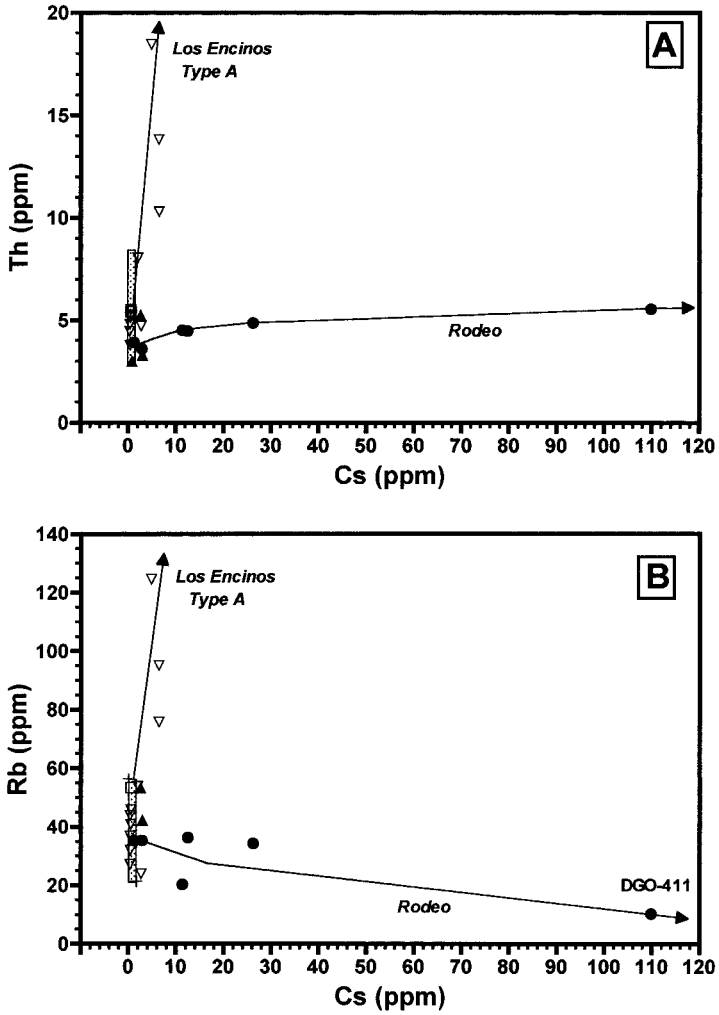

Figure 6. Whole-rock abundances of Cs vs. Th (A) and Rb (B) in Miocene volcanic rocks from the Mexican Basin and Range Province. The stippled field at 0–2 ppm Cs includes 50 Quaternary volcanic rocks from the Mexican Basin and Range Province (data sources as in Fig. 5). Crustal contamination trends for Rodeo and Los Encinos are indicated by arrows.

pered by the lack of data on local crustal rocks. Pb isotopic ratios of granulite and granite xenoliths and outcrops in northern México range from higher to much lower than those of Rodeo-Nazas samples (Fig. 8B). Contamination by crust with relatively radiogenic Pb, as depicted in model A (Fig. 8B) and inferred for the contamination trends of both Los Encinos and Parícutin (Fig. 8A), would indicate that the Rodeo samples are more contaminated than are Nazas samples, in contradiction to the Sr and Nd data. Contamination by crust with relatively unradiogenic Pb, as depicted in models B and C (Fig. 8B), would indicate that Rodeo samples are less contaminated, consistent with the Sr and Nd data.

Distinction between these two possibilities could help in evaluating the existence of the postulated Mojave-Sonora megashear or other major tectonic boundaries in México (Fig. 1; Anderson and Schmidt, 1983). The major area of crust with unradiogenic Pb is in Trans-Pecos Texas and Chihuahua, which underwent ca. 1.1 Ga (Grenville age) granulite facies metamorphism and concomitant U and Th depletion (Cameron et al., 1992; James and Henry, 1993). This Grenvillian crust is on the opposite, northeastern side of the Mojave-Sonora megashear (Fig. 1; Anderson and Schmidt, 1983) from Rodeo and Nazas. If the megashear truncated a southern continuation of North America, then the Precambrian belts of the southwestern United States should continue to the southwest but displaced southeastward by possibly 800 km (Anderson and Schmidt, 1983). Grenville-age crust similar to that of Texas and Chihuahua could underlie the Rodeo-Nazas area. Alternatively, if the megashear approximately coincides with an original southwestern edge of the North American continent (Stewart, 1988), the crust in Durango could be markedly different.

In contrast, Pb isotopic compositions of crustal rocks in Chihuahua and Sonora indicate a major west-northwest−trending tectonic boundary ~200 km north of Rodeo and Nazas, south of and slightly oblique to the Mojave Sonora megashear (Fig. 1; Housh and McDowell, 1999). North of this boundary many crustal rocks attain the unradiogenic Pb isotopic values that characterize Grenvillian and earlier crustal domains. South of the boundary, toward Rodeo and Nazas, unradiogenic Pb isotopic compositions are unusual. Data are sparse in this region, however, and Mesozoic intrusive rocks near Guanajuato,

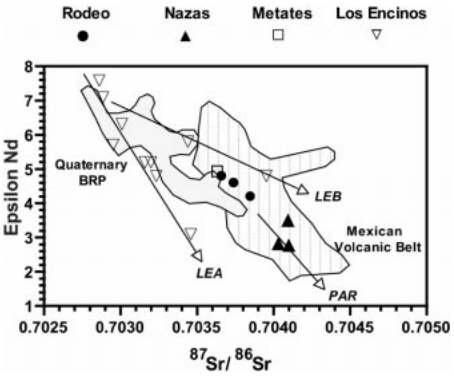

Figure 7. $^{87}Sr/^{86}Sr$ vs. ϵ_{Nd} showing initial values for the Miocene hawaiite suites of Rodeo and Nazas (Table 3), Metates (Aranda-Gómez et al., 1997), and Los Encinos (Luhr et al., 1995b). The field for the Quaternary Basin and Range Province (BRP) includes data for Ventura and Santo Domingo (Pier et al., 1989), La Breña (Pier et al., 1992), San Quintín (Luhr et al., 1995a), and Mesa Cacaxta (Aranda-Gómez et al., 1997). The field for the Mexican Volcanic Belt includes data from Colima, Tequila, Ceboruco, and San Juan (Verma and Luhr, 1993; Wallace and Carmichael, 1994; Luhr, 1997, 2000), Sangangüey and Tepetiltic (Verma and Nelson, 1989), Jorullo, Cerro La Pilita, and other vents from Michoacán-Guanajuato (Luhr, 1997), and Parícutin (Housh, unpublished data). Vectors for crustal contamination are shown for Los Encinos type A (LEA), Los Encinos type B (LEB), and Parícutin (PAR). Nazas samples appear to have undergone more crustal contamination than Rodeo samples. Estimates for the Sr and Nd isotopic compositions of the Mexican crust extend to higher $^{87}Sr/^{86}Sr$ and lower ϵ_{Nd} beyond the lower right corner of this plot, based on data for granulite xenoliths (Cameron et al., 1992; Ruiz et al., 1988; Roberts and Ruiz, 1989; Pier et al., 1992; Pier and Podosek, unpublished data) as well as granitic xenoliths and outcrops (McBirney et al., 1987; reanalyzed by Housh, unpublished data).

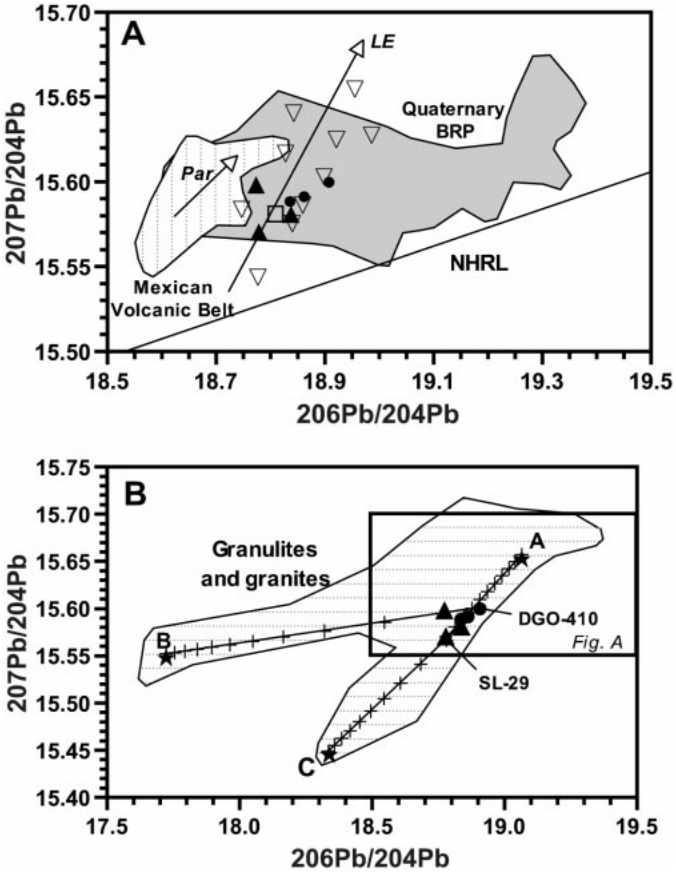

Figure 8. $^{206}Pb/^{204}Pb$ vs. $^{207}Pb/^{204}Pb$. (A) Initial values for the Miocene hawaiites of Rodeo and Nazas (Table 3), Metates, and Los Encinos, along with the field for Quaternary volcanic rocks from the Basin and Range Province (BRP) (data sources as in Fig. 7; Pier, 1989). Field for Mexican Volcanic Belt includes data for Colima, Ceboruco, San Juan, Mascota, Jorullo, Cerro La Pilita, El Chichón (Heatherington, 1988; Verma and Luhr, 1993; Luhr, 1997, 2000), and Parícutin (Par) (Housh, unpublished data). Crustal contamination vectors as in Figure 7. If crust beneath Rodeo and Nazas is like that beneath Los Encinos or Parícutin, vectors suggest that Rodeo samples have undergone more contamination than Nazas samples, the opposite of Sr-Nd data. NHRL is Northern Hemisphere Reference Line. (B) Small rectangle shows plot A. Field for granulites and granites includes granulite data from Cameron et al. (1992), Pier et al. (1992), and Pier and Podosek (unpublished data), along with granite data from Mango et al. (1991) and Housh (unpublished data). Lines to A, B, and C are possible mixing models between Rodeo-Nazas hawaiites and various crustal end members (stars); plus signs mark 10 wt% increments. Model A illustrates contamination of Nazas sample SL-29 with radiogenic crustal lead, represented by felsic granulite DGO-300E (5.0 ppm Pb) from the Durango volcanic field (Pier et al., 1992). Model B shows contamination of Rodeo sample DGO-410 with unradiogenic crustal lead at the lower limit of $^{206}Pb/^{204}Pb$, represented by orthogneiss GNX20 (15.3 ppm Pb) from La Olivina (Cameron et al., 1992). Model C depicts contamination of the same Rodeo sample DGO-410 with unradiogenic lead at the lower limit of $^{207}Pb/^{204}Pb$, represented by Mesozoic intrusive rock M/Gto3–89 (assumed to have 10 ppm Pb) from near the Rayas Mine in Guanajuato (Mango et al., 1991).

which are ~550 km southeast of Rodeo and Nazas, are unradiogenic (Mango et al., 1991).

Cs Enrichments in Miocene Volcanic Rocks and the Process of Crustal Contamination

Cs is a large, fluid-mobile alkali cation, the geochemical behavior of which is similar to that of K and Rb. Taylor and McLennan (1985) and Ben Othman et al. (1989) gave typical Cs abundances in important solar system and Earth reservoirs: CI chondritic meteorites, 279 ppb; primitive mantle, 18 ppb; oceanic crust, 30 ppb; ocean water, 0.3 ppb; river water, 0.02 ppb; suspended sediment in rivers, 6–21 ppm; pelagic clay, shale, graywacke, and argillite, 5–18 ppm; upper continental crust, 3.7 ppm; lower continental crust, 0.1 ppm; high-grade schists and gneisses, 2–125 ppm. It is clear from these estimates that rocks of Earth's continental crust hold 50–100 times as much Cs as those in Earth's mantle.

Accordingly, there is good reason to believe that Cs might be an excellent element to use to track crustal contamination of mantle-derived magmas (Hart and Reid, 1991). At the extreme end of this process are S-type granites and their volcanic equivalents, where enrichments of Cs result from partial melting of sedimentary crustal rocks. For example, the peraluminous Macusani rhyolites of Peru have Cs values that reach 566 ppm (Noble et al., 1984; Pichavant et al., 1988).

As discussed by Hart and Reid (1991), oceanic volcanic rocks have Rb/Cs values close to 85. Most Quaternary volcanic rocks from the Mexican Basin and Range Province have similarly high values (75 ± 20, 1σ; $n = 59$). Significantly lower values of Rb/Cs are found for the hawaiites from Rodeo (0.1–27.1), Nazas (14–41.7), and Los Encinos (8.5–94.7), supporting the interpretation that many of these Miocene hawaiites have interacted with continental crust, preferentially incorporating Cs relative to Rb and lowering their Rb/Cs values. Mineral-melt and mineral-fluid partitioning studies of Cs and Rb have shown that alkali feldspar and micas have to a 50-fold preference for Rb over Cs (Higuchi and Nagasawa, 1969; Volfinger, 1976; Villemant et al., 1981; Drexler et al., 1983; Mahood and Hildreth, 1983; Nash and Crecraft, 1985; Hart and Reid, 1991). As typical feldspathic schists move up metamorphic grade, Cs is progressively released through devolatization reactions (Bebout et al., 1999), so that by granulite grade, Cs concentrations are reduced to values of 1 ppm or less and Rb/Cs values are substantially elevated (Heier, 1973; Rudnick and Presper, 1990; Hart and Reid, 1991). These data indicate that fluids released during high-grade metamorphism can have correspondingly high Cs/Rb values. Thus, the process by which the Miocene hawaiites from the southern Basin and Range Province obtained their reduced Rb/Cs values may be complementary to the process of Rb/Cs elevation during high-grade metamorphic devolatization.

Important observations that cannot currently be reconciled with this interpretation are the following. (1) Rodeo sample DGO-411, which is richest in Cs, is also richest in Nb, Ta, Ba, La, Lu, Th, and U, and poorest in K and Rb. The enrichments of these incompatible elements are likely related to mineral-melt partitioning at low degrees of melting, but no known mineral-melt or mineral-fluid process can elevate Cs while it depletes Rb. (2) Many of the Rodeo samples are enriched in Cs and the Nazas samples are not, yet the Nazas samples have higher $^{87}Sr/^{86}Sr$ and lower ϵ_{Nd} than the Rodeo samples. (3) Trends among Cs, Rb, and Th are very different for Rodeo-Nazas hawaiites compared to those from Los Encinos, yet both presumably resulted from crustal contamination.

Magma Evolution in Relation to the Evolving Tectonic Setting

The following discussion attempts to relate the pattern of intraplate magmatism in the southern Basin and Range Province to the evolving tectonic and thermal state of the lithosphere. A transition from east-northeast compression to east-northeast extension probably occurred ca. 32 Ma in the southern Basin and Range Province of México and Texas (Henry et al., 1991; Henry and Aranda-Gomez, 1992), consistent with the 32.3–30.6 Ma initiation of extension around Rodeo and Nazas. Extension began at about the same time as the main Oligocene flare-up of Sierra Madre Occidental ignimbrite volcanism (28–32 Ma; McDowell and Keizer, 1977; Swanson et al., 1978; McDowell and Clabaugh, 1979). Intraplate-type, mafic alkalic magmas, characterized by enrichments of Ti, Nb, and Ta, may have begun to ascend beneath this region as extension started. However, heating of the lithosphere during the ignimbrite flare-up would have lowered the density of the crust and upper mantle and raised the brittle-ductile transition. Deeply penetrating brittle structures that would transport magma quickly to the surface probably would not have formed at this time, so magmas instead ascended slowly, losing heat as they crystallized as differentiated gabbroic plutons in the lower crust. Intraplate-type magmas first erupted ca. 29 Ma in Trans-Pecos Texas, where ignimbritic volcanism was far less intense than in the Sierra Madre Occidental. Further lithospheric cooling and descent of the brittle-ductile transition may have allowed subsequent hawaiite magmas (ca. 24 Ma; Texas, Rodeo-Nazas; ca. 14–11 Ma; Los Encinos and Metates) to rise more efficiently toward the surface, and in doing so they disrupted the earlier plutons to form their entrained megacrysts. The differentiated, crustally contaminated nature of these 24–11 Ma hawaiites indicates that they still underwent considerable heat loss, crystallization, and crustal interaction during ascent. The evolved, plutonic megacrysts present within these early extensional hawaiites throughout the Mexican and Texas Basin and Range Province may reveal the fate of the earliest generated (ca. 30–26 Ma?), but never-erupted intraplate magmas.

Pliocene−Quaternary volcanic fields are dominated by related, but more primitive intraplate-type magmas, many of which carried large, deep-crustal and upper mantle xenoliths. These younger magmas appear to have ascended rapidly and undergone little differentiation and crustal contamination. We suggest that this change is a consequence of further lithospheric cooling and descent of the brittle-ductile transition to greater depths long after the ignimbrite flare-up. Brittle structures were able to penetrate to greater depths, which, coupled with the evolving extensional stress field, allowed extremely efficient magmatic ascent.

Miocene Hawaiites as Probes of Their Mantle Source Regions

One of the goals of our studies in the southern Basin and Range Province is to understand geodynamic processes in the underlying mantle that accompanied and perhaps controlled rift development. For the United States portion of the Basin and Range Province, earlier workers used temporal changes in elemental abundances and Sr and Nd isotopic compositions of mafic volcanic rocks to infer that magma source regions shifted over time, from shallow lithospheric mantle to deeper convecting asthenospheric mantle (Perry et al., 1987, 1988; Fitton et al., 1991; Daley and DePaolo, 1992; Bradshaw et al., 1993). In order to draw such conclusions, it is essential to demonstrate that the geochemistry of the volcanic rocks faithfully records conditions in the mantle source region, i.e., that they truly act as probes of the mantle. The early Miocene Rodeo-Nazas hawaiites have trace element characteristics (e.g., similar concentrations to ocean-island basalts, with peaks at Nb and Ta on spidergrams; Fig. 5) that are generally attributed to asthenospheric mantle sources. In contrast, magmas derived from the asthenosphere were interpreted to only appear during the past 5–10 m.y. in the United States portion of the Basin and Range Province (Perry et al., 1987; Fitton et al., 1991; Bradshaw et al., 1993). However, the early Miocene (Rodeo-Nazas) and middle Miocene (Los Encinos and Metates) hawaiites from the southern Basin and Range Province mostly have the enriched Sr and Nd isotopic compositions that are assumed to indicate involvement of shallower lithospheric mantle source regions. For example, Perry et al. (1987) correlated ϵ_{Nd} values of $+7$ and $+8$ to the asthenosphere and values of 0 to $+2$ to the lithosphere. They interpreted alkali basalts with intermediate values ($+3.3$ to $+6.6$, similar to those from Rodeo-Nazas) to have been derived by partial melting from the asthenosphere-lithosphere boundary. However, the differentiated nature of the southern Basin and Range Province hawaiites, plus strong geochemical evidence of crustal contamination in the form of elevated concentra-

tions of Cs and reduced Rb/Cs values, should caution against this simple interpretation. We consider it more likely that the enriched Sr and Nd isotopic signatures of these Miocene hawaiites also reflect crustal contamination. Thus, differentiation and contamination during ascent through the crust appear to have obscured many of the geochemical signatures of the mantle source regions for these early extensional magmas, severely compromising their use as probes of the mantle. Similar cautions about cryptic crustal contamination of mafic magmas have been raised before (Doe et al., 1969; Glazner and Farmer, 1992; Baldridge et al., 1996). In the middle Miocene Los Encinos suite (Luhr et al., 1995b), a complete spectrum of hawaiites is present, from apparently uncontaminated types to others affected by two different forms of crustal contamination. The uncontaminated Miocene hawaiites from Los Encinos do not show lithospheric signatures in Sr and Nd isotopic ratios. Rather, they have lower $^{87}Sr/^{86}Sr$ and higher ϵ_{Nd} than any of the Quaternary intraplate-type rocks (Fig. 7). We conclude that no evidence exists for a temporal shift from lithospheric to asthenospheric mantle sources during evolution of the Mexican Basin and Range Province.

ACKNOWLEDGMENTS

Our investigation built on earlier studies by Gerardo Aguirre-Díaz and Fred McDowell, who generously shared specimens and data. The original manuscript was improved by the critical review comments of Ken Cameron, Wendy Bohrson, Lang Farmer, and Allen Glazner, who have our thanks. This work was supported by Consejo Nacional de Ciencia y Tecnología (CONACYT, México) grant 3657P-T9608 to Aranda-Gómez and by the Sprague Endowment of the Smithsonian Institution.

REFERENCES CITED

Aguirre-Díaz, G.J., and McDowell, F.W., 1991, The volcanic section at Nazas, Durango, México, and the possibility of widespread Eocene volcanism within the Sierra Madre Occidental: Journal of Geophysical Research, v. 96, no. B8, p. 13373–13388.

Aguirre-Díaz, G.J., and McDowell, F.W., 1993, Nature and timing of faulting and synextensional magmatism in the southern Basin and Range, central-eastern Durango, México: Geological Society of America Bulletin, v. 105, p. 1435–1444.

Anderson, T.H., and Schmidt, V.A., 1983, The evolution of middle America and the Gulf of Mexico−Caribbean Sea region during Mesozoic time: Geological Society of America Bulletin, v. 94, p. 941–966.

Angelier, J., 1979, Determination of the mean principal stress for a given fault population: Tectonophysics, v. 56, p. 17–26.

Aranda-Gómez, J.J., and Henry, C.D., 1992, Fallamiento cuarternario cerca de la ciudad de Durango, naturaleza del período de deformación más joven relacionado a extensión multiepisódica en el noroeste de México: Geos, v. 12, p. 53–54.

Aranda-Gómez, J.J., Henry, C.D., Luhr, J.F., and McDowell, F.W., 1997, Cenozoic volcanism and tectonics in NW México—A transect across the Sierra Madre Occidental volcanic field and observations on extension related magmatism in the southern Basin and Range and Gulf of California tectonic provinces, *in* Aguirre-Díaz, G.J., et al., eds., Magmatism and tectonics in central and northwestern México—A selection of the 1997 IAVCEI General Assembly excursions: Universidad Nacional Autónoma de México, Instituto de Geología, México, D.F., Excursión 11, p. 41–84.

Baldridge, W.S., Sharp, Z.D., and Reid, K.D., 1996, Quartz-bearing basalts: Oxygen isotopic evidence for crustal contamination of continental mafic rocks: Geochimica et Cosmochimica Acta, v. 60, p. 4765–4772.

Bartolini, C., Damon, P.E., Shafiqullah, M., and Morales M., 1995, Geochronologic contributions to the Tertiary sedimentary-volcanic sequences (''Baucarit Formation'') in Sonora, México: Geofísica Internacional, v. 34, p. 67–77.

Bebout, G.E., Ryan, J.G., Leeman, W.P., and Bebout, A.E., 1999, Fractionation of trace elements by subduction-zone metamorphism—Effect of convergent margin thermal evolution: Earth and Planetary Science Letters, v. 171, p. 63–81.

Ben Othman, D., White, W.M., and Patchett, J., 1989, The geochemistry of marine sediments, island arc magma genesis, and crust-mantle recycling: Earth and Planetary Science Letters, v. 94, p. 1–21.

Berger, G., Schott, J., and Guy, C., 1988, Behavior of Li, Rb, and Cs during basalt glass and olivine dissolution and chlorite, smectite, and zeolite precipitation from seawater: Experimental investigations and modelization between 50 degrees and 300 degrees C: Chemical Geology, v. 71, p. 297–312.

Bonneau, M., 1970, Una nueva area Cretacica fosilifera en el estado de Sinaloa: Boletín de la Sociedad Geológica Mexicana, v. 32, p. 159–167.

Bradshaw, T.K., Hawkesworth, C.J., and Gallagher, K., 1993, Basaltic volcanism in the southern Basin and Range: No role for a mantle plume: Earth and Planetary Science Letters, v. 116, p. 45–62.

Cameron, K.L., Robinson, J.V., Niemeyer, S., Nimz, G.J., Kuentz, D.C., Harmon, R.S., Bohlen, S.R., and Collerson, K.D., 1992, Contrasting styles of pre-Cenozoic and mid-Tertiary crustal evolution in northern México: Evidence from deep crustal xenoliths from La Olivina: Journal of Geophysical Research, v. 97, p. 17353–17376.

Daley, E.E., and DePaolo, D.J., 1992, Isotopic evidence for lithospheric thinning during extension: Southeastern Great Basin: Geology, v. 20, p. 104–108.

Deino, A., and Potts, R., 1990, Single-crystal $^{40}Ar/^{39}Ar$ dating of the Olorgesailie Formation, southern Kenya Rift: Journal of Geophysical Research, v. 95, p. 8453–8470.

Doe, B.R., Lipman, P.W., and Hedge, C.E., 1969, Primitive and contaminated basalts from the southern Rocky Mountains, U.S.A.: Contributions to Mineralogy and Petrology, v. 21, p. 142–156.

Drexler, J.W., Bornhorst, T.J., and Noble, D.C., 1983, Trace-element sanidine/glass distribution coefficients for peralkaline silicic rocks and their implications to peralkaline petrogenesis: Lithos, v. 16, p. 265–271.

Enciso-De La Vega, S., 1963, Hoja Nazas, Resumen de las geologia de la Hoja Nazas, estado de Durango, Carta Geologico México, Hoja Nazas, 13-k(6): Universidad Nacional Autónoma de México, Instituto de Geología, México, D.F., scale 1:100 000.

Fitton, J.G., James, D., and Leeman, W.P., 1991, Basic magmatism associated with late Cenozoic extension in the western United States: Compositional variations in space and time: Journal of Geophysical Research, v. 96, p. 13693–13711.

Gans, P.B., 1997, Large-magnitude Oligo-Miocene extension in southern Sonora: Implications for the tectonic evolution of northwest México: Tectonics, v. 16, p. 388–408.

Glazner, A.F., and Farmer, G.L., 1992, Production of isotopic variability in continental basalts by cryptic crustal contamination: Science, v. 255, p. 72–74.

Hart, S.R., 1969, K, Rb, Cs contents and K/Rb, K/Cs ratios of fresh and altered submarine basalts: Earth and Planetary Science Letters, v. 6, p. 295–303.

Hart, S.R., 1984, A large-scale isotope anomaly in the Southern Hemisphere mantle: Nature, v. 309, p. 753–757.

Hart, S.R., and Reid, M.R., 1991, Rb/Cs fractionation: A link between granulite metamorphism and the S-process: Geochimica et Cosmochimica Acta, v. 55, p. 2379–2383.

Heatherington, A.L., 1988, Isotopic systematics of volcanics from south-central Rio Grande Rift and the western Mexican Volcanic Belt: Implications for magmatic and tectonic evolution of Cenozoic extensional regimes in western North America [Ph.D. dissert.]: St. Louis, Missouri, Washington University, 207 p.

Heier, K.S., 1973, Geochemistry of granulite facies rocks and problems of their origin: Royal Society of London Philosophical Transactions, ser. A, v. 273, p. 429–442.

Henry, C.D., and Aranda-Gómez, J.J., 1992, The real southern Basin and Range: Mid- to late Cenozoic extension in México: Geology, v. 20, p. 701–704.

Henry, C.D., and Aranda-Gómez, J.J., 2000, Plate interactions control middle-late Miocene, proto-Gulf and Basin and Range extension in the southern Basin and Range: Tectonophysics, v. 318, p. 1–26.

Henry, C.D., and Fredrikson, G., 1987, Geology of southern Sinaloa adjacent to the Gulf of California: Geological Society of America Map and Chart Series MCH063, 14 p., scale 1:250 000.

Henry, C.D., and Price, J.G., 1986, Early Basin and Range development in Trans-Pecos Texas and adjacent Chihuahua: Magmatism and orientation, and timing and style of extension: Journal of Geophysical Research, v. 91, p. 6213–6224.

Henry, C.D., Price, J.G., and James, E.W., 1991, Mid-Cenozoic stress evolution and magmatism in the southern Cordillera, Texas and México: Transition from continental arc to intraplate extension: Journal of Geophysical Research, v. 96, p. 13545–13560.

Higuchi, H., and Nagasawa, H., 1969, Partition of trace elements between rock-forming minerals and the host volcanic rocks: Earth and Planetary Science Letters, v. 7, p. 281–287.

Housh, T., and McDowell, F.W., 1999, Delineation of basement provinces in northwestern México through isotopic studies of Late Cretaceous to mid-Tertiary igneous rocks: Eos (Transactions, American Geophysical Union), v. 80, p. F987.

Instituto Nacional de Estadistica Geografia e Informatica, 1988, Santiago Papasquiaro: Mexico City, Carta Geologica G13–8, scale 1:250 000.

James, E.W., and Henry, C.D., 1991, Compositional changes in Trans-Pecos Texas magmatism coincident with Cenozoic stress realignment: Journal of Geophysical Research, v. 96, p. 13561–13575.

James, E.W., and Henry, C.D., 1993, Southeastern extent of the North American craton in Texas and northern Chihuahua as revealed by Pb isotopes: Geological Society of America Bulletin, v. 105, p. 116–126.

Jochum, K.P., and Verma, S.P., 1996, Extreme enrichment of Sb, Tl, and other trace elements in altered MORB: Chemical Geology, v. 130, p. 289–299.

Kerr, D.R., and Kidwell, S.M., 1991, Late Cenozoic sedimentation and tectonics, western Salton Trough, California, *in* Walawender, M.J., and Hanan, B.J., eds., Geological excursions in southern California and México, Guidebook, Geological Society of America Annual Meeting: San Diego, California, Department of Geological Sciences, San Diego State University, p. 397–416.

Korotev, R.L., 1996, A self-consistent compilation of elemental concentration data for 93 geochemical reference samples: Geostandards Newsletter, v. 20, p. 217–245.

Le Bas, M.J., Le Maitre, R.W., Streckeisen, A., and Zanettin, B., 1986, A chemical classification of volcanic rocks based on the total alkali-silica diagram: Journal of Petrology, v. 27, p. 745–750.

Lindstrom, D.J., and Korotev R.L., 1982, TEABAGS: Computer programs for instrumental neutron activation analysis: Journal of Radioanalytical Chemistry, v. 70, p. 439–458.

Luhr, J.F., 1997, Extensional tectonics and diverse primitive volcanic rocks in the western Mexican Volcanic Belt: Canadian Mineralogist, v. 35, p. 473–500.

Luhr, J.F., 2000, The geology and petrology of Volcán San Juan (Nayarit, México) and the compositionally zoned Tepic Pumice: Journal of Volcanology and Geothermal Research, v. 95, p. 109–156.

Luhr, J.F., Aranda-Gómez, J.J., and Pier, J.G., 1989, Spinel-lherzolite-bearing Quaternary volcanic centers in San Luis Potosí, México: 1. Geology, mineralogy, and petrology: Journal of Geophysical Research, v. 94, p. 7916–7940.

Luhr, J.F., Aranda-Gómez, J.J., and Housh, T.B., 1995a, The San Quintín Volcanic Field, Baja California Norte, México: Geology, petrology, and geochemistry: Journal of Geophysical Research, v. 100, no. B7, p. 10353–10380.

Luhr, J.F., Pier, J.G., Aranda-Gómez, J.J., and Podosek, F.A., 1995b, Crustal contamination in early Basin-and-Range hawaiites of the Los Encinos Volcanic Field, central México: Contributions to Mineralogy and Petrology, v. 118, p. 321–339.

Mahood, G., and Hildreth, W., 1983, Large partition coefficients for trace elements in high-silica rhyolites: Geochimica et Cosmochimica Acta, v. 47, p. 11–30.

Mango, H., Zantop, H., and Oreskes, N., 1991, A fluid inclusion and isotope study of the Rayas Ag-Au-Cu-Pb-Zn mine, Guanajuato, México: Economic Geology, v. 86, p. 1554–1561.

McBirney, A.R., Taylor, H.P., Jr., and Armstrong, R.L., 1987, Parícutin re-examined: A classic example of crustal assimilation in calc-alkaline magma: Contributions to Mineralogy and Petrology, v. 95, p. 4–20.

McDowell, F.W., 1983, K-Ar dating: Incomplete extraction of radiogenic argon from alkali feldspar: Isotope Geoscience, v. 1, p. 119–126.

McDowell, F.W., and Clabaugh, S.E., 1979, Ignimbrites of the Sierra Madre Occidental and their relation to the tectonic history of western México: Geological Society of America Special Paper 180, p. 113–124.

McDowell, F.W., and Keizer, R.P., 1977, Timing of mid-Tertiary volcanism in the Sierra Madre Occidental between Durango City and Mazatlan, México: Geological Society of America Bulletin, v. 88, p. 1479–1486.

McDowell, F.W., and Mauger, R.L., 1994, K-Ar and U-Pb zircon chronology of Late Cretaceous and Tertiary magmatism in central Chihuahua State, Mexico: Geological Society of America Bulletin, v. 106, p. 118–132.

McDowell, F.W., Roldán-Quintana, J., and Amaya Martínez, R., 1997, Interrelationship of sedimentary and volcanic deposits associated with Tertiary extension in Sonora, México: Geological Society of America Bulletin, v. 109, p. 1349–1360.

McIntosh, W.C., and Chamberlin, R.M., 1994, $^{40}Ar/^{39}Ar$ geochronology of middle to late Cenozoic ignimbrites, mafic lavas, and volcaniclastic rocks in the Quemado region, New Mexico: New Mexico Geological Society Guidebook, v. 45, p. 165–185.

Moore, G., Marone, C., Carmichael, I.S.E., and Renne, P., 1994, Basaltic volcanism and extension near the intersection of the Sierra Madre volcanic province and the Mexican Volcanic Belt: Geological Society of America Bulletin, v. 106, p. 383–394.

Morton, J.P., 1985, Rb-Sr evidence for punctuated illite/smectite diagenesis in the Oligocene Frio Formation, Texas Gulf Coast: Geological Society of America Bulletin, v. 96, p. 114–122.

Morton, J.P., and Long, L.E., 1980, Rb-Sr dating of Paleozoic glauconite from the Llano region, central Texas: Geochimica et Cosmochimica Acta, v. 44, p. 663–672.

Nash, W.P., and Crecraft, H.R., 1985, Partition coefficients for trace elements in silicic magmas: Geochimica et Cosmochimica Acta, v. 49, p. 2309–2322.

Nelson, D.O., and Schieffer, J.H., 1990, Ultramafic inclusions and megacrysts in mafic rocks of the Terlingua district, West Texas, *in* Dickerson, P.W., et al., eds., Geology of the Big Bend and Trans-Pecos region, Fieldtrip guidebook: San Antonio, South Texas Geological Society, p. 211–249.

Nieto-Samaniego, A.F., Ferrari, L., Alaniz-Alvarez, S.A., Labarthe-Hernández, G., and Rosas-Elguera, R., 1999, Variation of Cenozoic extension and volcanism across the southern Sierra Madre Occidental volcanic province, México: Geological Society of America Bulletin, v. 111, p. 347–363.

Noble, D.C., Vogel, T.A., Peterson, P.S., Landis, G.P., Grant, N.K., Jezek, P.A., and McKee, E.H., 1984, Rare-element-enriched, S-type ash-flow tuffs containing phenocrysts of muscovite, andalusite, and sillimanite, southeastern Peru: Geology, v. 12, p. 35–39.

Nourse, J.A., Anderson, T.A., and Silver, L.T., 1994, Tertiary metamorphic core complexes in Sonora, northwestern México: Tectonics, v. 13, p. 1161–1182.

Peck, L.C., 1964, Systematic analysis of silicates: U.S. Geological Survey Bulletin, v. 1170, 89 p.

Perry, F.V., Baldridge, W.S., and DePaolo, D.J., 1987, Role of asthenosphere and lithosphere in the genesis of late Cenozoic basaltic rocks from the Rio Grande Rift and adjacent regions of the southwestern United States: Journal of Geophysical Research, v. 92. p. 9193–9213.

Perry, F.V., Baldridge, W.S., and DePaolo, D.J., 1988, Chemical and isotopic evidence for lithospheric thinning beneath the Rio Grande rift: Nature, v. 332, p. 432–434.

Pichavant, M., Kontak, D.J., Briqueu, L., Valencia, H.J., and Clark, A.H., 1988, The Miocene-Pliocene Macusani Volcanics, SE Peru: 2, Geochemistry and origin of a felsic peraluminous magma: Contributions to Mineralogy and Petrology, v. 100, p. 325–338.

Pier, J.G., 1989, Isotope and trace element systematics in a spinel-lherzolite-bearing suite of basanitic volcanic rocks from San Luis Potosí, México [Ph.D. dissert.]: St. Louis, Missouri, Washington University, 316 p.

Pier, J.G., Podosek, F.A., Luhr, J.F., Brannon, J.C., and Aranda-Gómez, J.J., 1989, Spinel-lherzolite−bearing Quaternary volcanic centers of San Luis Potosí, México: II. Sr and Nd isotopic systematics: Journal of Geophysical Research, v. 94, no. B6, p. 7941–7951.

Pier, J.G., Luhr, J.F., Podosek, F.A., and Aranda-Gómez, J.J., 1992, The La Breña−El Jagüey Maar Complex, Durango, México: II. Petrology and geochemistry: Bulletin of Volcanology, v. 54, p. 405–428.

Roberts, S.J., and Ruiz, J., 1989, Geochemistry of exposed granulite facies terrains and lower crustal xenoliths in México: Journal of Geophysical Research, v. 94, no. B6, p. 7961–7974.

Rudnick, R.L., and Presper, T., 1990, Geochemistry of intermediate- to high-pressure granulites, *in* Vielzeuf, D., and Vidal, Ph., eds., Granulites and crustal evolution: Dordrecht, Kluwer Academic Publishers, p. 523–550.

Ruiz, J., Patchett, P.J., and Arculus, R.J., 1988, Nd-Sr isotope composition of lower crustal xenoliths—Evidence for the origin of mid-Tertiary felsic volcanics in México: Contributions to Mineralogy and Petrology, v. 99, p. 36–43.

Samson, S.D., and Alexander, E.C., Jr., 1987, Calibration of the interlaboratory $^{40}Ar/^{39}Ar$ dating standard, MMhb-1: Chemical Geology, v. 66, p. 27–34.

Smith, J.A., 1989, Extension-related magmatism of the Durango Volcanic Field, Durango, México [Master's thesis]: St. Louis, Missouri, Washington University, 102 p.

Spencer, J.E., and Reynolds, S.J., 1989, Middle Tertiary tectonics of Arizona and adjacent areas, *in* Jenney, J.P., and Reynolds, S.J., eds., Geologic evolution of Arizona: Arizona Geological Society Digest, v. 17, p. 539–574.

Spencer, J.E., Richard, S.M., Reynolds, S.J., Miller, R.J., Shafiqullah, M., Gilbert, W.G., and Grubensky, M.J., 1995, Spatial and temporal relationships between mid-Tertiary magmatism and extension in southwestern Arizona: Journal of Geophysical Research, v. 100, p. 10321–10351.

Steiger, R.H., and Jäger, E., 1977, Subcommission on geochronology: Convention on the use of decay constants in geo- and cosmochronology: Earth and Planetary Science Letters, v. 36, p. 359–362.

Stewart, J.H., 1988, Latest Proterozoic and Paleozoic southern margin of North America and the accretion of México: Geology, v. 16, p. 186–189.

Stewart, J.H., and Roldán-Quintana, J., 1994, Map showing late Cenozoic extensional tilt patterns and associated structures in Sonora and adjacent areas: U.S. Geological Survey Miscellaneous Field Studies Map MF-2238, scale 1:1 000 000.

Stewart, J.H., Anderson, R.E., Aranda-Gómez, J.J., Beard, L.S., Billingsley, G.H., Cather, S.M., Dilles, J.H., Dokka, R.K., Faulds, J.E., Ferrari, L., Grose, T.L.T., Henry, C.D., Janecke, S.U., Miller, D.M., Richard, S.M., Rowley, P.D., Roldan-Quintana, J., Scott, R.B., Sears, J.W., and Williams, V.S., 1998, Map showing Cenozoic tilt domains and associated structural features, western North America, *in* Faulds, J.E., and Stewart, J.H., eds., Accommodation zones and transfer zones: Regional segmentation of the Basin and Range Province: Geological Society of America Special Paper 323, Plate 1.

Swanson, E.R., Keizer, R.P., Lyons, J.I., and Clabaugh, S.E., 1978, Tertiary volcanism and caldera development near Durango City, Sierra Madre Occidental, México: Geological Society of America Bulletin, v. 89, p. 1000–1012.

Taylor, S.R., and McLennan, S.M., 1985, The continental crust: Its composition and evolution: Oxford, Blackwell, 312 p.

Verma, S.P., and Luhr, J.F., 1993, Sr-Nd-Pb isotope and trace element geochemistry of calc-alkaline andesites from Volcán Colima, México: Geofísica Internacional, v. 32, p. 617–631.

Verma, S.P., and Nelson, S.A., 1989, Isotopic and trace element constraints on the origin and evolution of alkaline and calc-alkaline magmas in the northwestern Mexican Volcanic Belt: Journal of Geophysical Research, v. 94, p. 4531–4544.

Villemant, B., Jaffrezic, H., Joron, J.-L., and Treuil, M., 1981, Distribution coefficients of major and trace elements; fractional crystallization in the alkali basalt series of Chaîne de Puys (Massif Central, France): Geochimica et Cosmochimica Acta, v. 45, p. 1997–2016.

Volfinger, M., 1976, Effet de la tempérture sur les distributions de Na, Rb, et Cs entre la sanidine, la muscovite, la phlogopite et une solution hydrothermale sous une pression de 1 kbar: Geochimica et Cosmochimica Acta, v. 40, p. 267–282.

Wallace, P., and Carmichael, I.S.E., 1994, Petrology of Volcán Tequila, Jalisco, México: Disequilibrium phenocryst assemblages and evolution of the subvolcanic magma system: Contributions to Mineralogy and Petrology, v. 117, p. 345–361.

Wilshire, J.G., and Shervais, J.W., 1975, Al-augite and Cr-diopside ultramafic xenoliths in basaltic rocks from western United States: Physics and Chemistry of the Earth, v. 9, p. 257–272.

Wood, D.A., Tarney, J., and Weaver, B.L., 1981, Trace element variations in Atlantic Ocean basalts and Proterozoic dykes from Northwest Scotland: Their bearing upon the nature and geochemical evolution of the upper mantle: Tectonophysics, v. 75, p. 91–112.

MANUSCRIPT RECEIVED BY THE SOCIETY AUGUST 10, 1999
REVISED MANUSCRIPT RECEIVED MAY 1, 2000
MANUSCRIPT ACCEPTED JULY 10, 2000

Printed in the USA